



ECOLE
POLYTECHNIQUE
DE BRUXELLES

UNIVERSITÉ LIBRE DE BRUXELLES

SUMMARY

Turbomachinery
MECA-H-402

Author:
Enes ULUSOY

Professor:
Patrick HENDRICK

Year 2016 - 2017

Appel à contribution

Synthèse Open Source



Ce document est grandement inspiré de l'excellent cours donné par Patrick HENDRICK à l'EPB (École Polytechnique de Bruxelles), faculté de l'ULB (Université Libre de Bruxelles). Il est écrit par les auteurs susnommés avec l'aide de tous les autres étudiants et votre aide est la bienvenue ! En effet, il y a toujours moyen de

l'améliorer surtout que si le cours change, la synthèse doit être changée en conséquence. On peut retrouver le code source à l'adresse suivante

<https://github.com/nenglebert/Syntheses>

Pour contribuer à cette synthèse, il vous suffira de créer un compte sur *Github.com*. De légères modifications (petites coquilles, orthographe, ...) peuvent directement être faites sur le site ! Vous avez vu une petite faute ? Si oui, la corriger de cette façon ne prendra que quelques secondes, une bonne raison de le faire !

Pour de plus longues modifications, il est intéressant de disposer des fichiers : il vous faudra pour cela installer L^AT_EX, mais aussi *git*. Si cela pose problème, nous sommes évidemment ouverts à des contributeurs envoyant leur changement par mail ou n'importe quel autre moyen.

Le lien donné ci-dessus contient aussi un README contenant de plus amples informations, vous êtes invités à le lire si vous voulez faire avancer ce projet !

Licence Creative Commons

Le contenu de ce document est sous la licence Creative Commons : *Attribution-NonCommercial-ShareAlike 4.0 International (CC BY-NC-SA 4.0)*. Celle-ci vous autorise à l'exploiter pleinement, compte-tenu de trois choses :



1. *Attribution* ; si vous utilisez/modifiez ce document vous devez signaler le(s) nom(s) de(s) auteur(s).
2. *Non Commercial* ; interdiction de tirer un profit commercial de l'œuvre sans autorisation de l'auteur
3. *Share alike* ; partage de l'œuvre, avec obligation de rediffuser selon la même licence ou une licence similaire

Si vous voulez en savoir plus sur cette licence :

<http://creativecommons.org/licenses/by-nc-sa/4.0/>

Merci !

Contents

1	Fundamental equations of turbomachinery	1
1.1	Basics and principles	1
1.1.1	Introduction	1
1.1.2	Classification of turbomachines	1
1.1.3	General organization of turbomachines	1
1.1.4	Notations	2
1.1.5	Velocity triangle	2
1.2	Fundamental equations of the flow	2
1.2.1	Equations of the flow in a fixed frame	2
1.2.2	Equations of the flow in a moving frame	3
1.3	Fundamental equations of turbomachinery	4
1.3.1	Compressors	4
1.3.2	Detailed power distribution	7
1.4	Turbines	7
1.5	Axial thrust and disc friction	8
1.5.1	Definition	8
1.5.2	Equation of the axial thrust	8
1.5.3	Friction of the disc	9
2	Centrifugal pumps	10
2.1	Generalities	10
2.1.1	Description - Type of turbopump	10
2.1.2	Installation of a turbopump	10
2.1.3	Energy developed by the turbopump - flow rate	11
2.1.4	Useful power or hydraulic power	11
2.1.5	Working point of a turbopump	11
2.1.6	Characteristic of the hydraulic circuit	11
2.1.7	Performance curve of a pump	12
2.1.8	Working regimes	12
2.1.9	Practical units	12
2.2	The centrifugal pump	12
2.2.1	Organization of a centrifugal pump	12
2.2.2	The distributor	12
2.2.3	The rotor	12
2.2.4	Number and shape of the blades	13
2.2.5	Head of Euler of the rotor	13
2.2.6	Losses in the rotor due to friction	14
2.2.7	Loss due to the internal leak flow	14
2.2.8	Friction of the disc on the non-active fluid	14

2.2.9	The diffuser	15
2.2.10	The volute or collector	16
2.2.11	Characteristic curves of a centrifugal pump	16
2.3	Performance curves of centrifugal pumps non-dimensional analysis	16
2.3.1	Theory of Vachy-Buckingham	16
2.3.2	Application to turbopumps	17
2.3.3	Performance curves of a type of pumps	17
2.3.4	Characteristic curves of a pump	17
2.3.5	Stability of a turbopump	17
2.3.6	Pump cavitation	18
2.4	The network and its characteristic curve	19
2.4.1	Simple circuit	19
2.4.2	Calculation of the characteristic curve of a circuit	19
2.5	Selection of a pump of a pump type	20
2.5.1	Users of pumps	20
2.5.2	General case	21
2.5.3	Choice of the pump type	21
2.5.4	Choice of the pump	21
2.5.5	Groups of pumps	21
3	Axial turbines	23
3.1	Stages of axial turbines	23
3.1.1	Organization of a stage - 2D flow	23
3.2	Impulse stage with one velocity drop	24
3.2.1	Definition of the stage	24
3.2.2	Evolution of the gas/steam - Velocity triangles	24
3.2.3	Power on the wheel shaft (P_R)	26
3.2.4	Degree of reaction	26
3.2.5	Stage efficiency – Pre-design	27
3.2.6	Performance in off-design condition	28
3.2.7	Pressure drop in the optimum conditions	29
3.3	Impulse stage with two velocity drops or two-stage impulse turbine	29
3.3.1	Need for two velocity drop	29
3.3.2	Organization and way of working	29
3.3.3	Evolution of the fluid – velocity triangles	30
3.3.4	Power P_R on the rotor	31
3.3.5	Stage efficiency – Pre-design of the stage	31
3.3.6	Performance of an existing stage in off-design conditions	32
3.3.7	Optimum speed coefficient and pressure drop	32
3.4	Impulse stage with three velocity drops	32
3.4.1	Comparison between the three types of impulse stages	32
3.5	Turbine reaction stage	33
3.5.1	Organization	33
3.5.2	Transformations and velocity triangles	33
3.5.3	Losses - Recovery	34
3.5.4	Power delivered to the rotor	34
3.5.5	Degree of reaction	35
3.5.6	Parsons turbine reaction stage	35
3.5.7	Degree of reaction of Parsons turbine - Enthalpy drop	35

3.5.8	Stage efficiency and pre-design study	36
3.5.9	Off-design operation of the stage	36
3.6	Comparative study of the stage types	37
3.6.1	Optimum velocity coefficient	37
3.6.2	Stage efficiency	37
4	Hydraulic turbines	38
4.1	Introduction	38
4.1.1	Definition	38
4.1.2	Basic notions	38
4.1.3	Mechanical power turbine shaft	39
4.1.4	Efficiency of a turbine	39
4.1.5	Specific speed of a turbine	39
4.2	Impulse turbines	39
4.2.1	Pelton turbines	39
4.2.2	Cross-flow or Banki-Mitchell turbines	40
4.3	Reaction turbines	40
4.3.1	Francis turbines	41
4.3.2	Propeller and Kaplan turbines	41
4.3.3	Inverted pumps	42
4.3.4	Archimedes turbines	42
4.4	Performance curves and operating conditions	43
4.4.1	Implementation of a hydroturbine	43
4.4.2	Turbine generator group layout	43
4.5	Summary	44

Chapter 1

Fundamental equations of turbomachinery

1.1 Basics and principles

1.1.1 Introduction

About the exam, he likes the drawings and likes to give a sentence and asks if it is the reality or not. The questions are about the **lectures** and not the notes. This summary is thus mainly based on the lectures.

The course is organized as:

1. **Turbopumps** and the system involved: a pump is something applying pressure to a fluid $\Delta p > 0$, which will first be a liquid $\rho = cst$.
2. **Turbines**: in this case the fluid involves a pressure loss $\Delta p < 0$, so expansion (a valve, simple releaser). We will see the gas turbines and the hydraulic turbines. Some machines can be used in the two ways, both roles, same mechanical component is acting as a pump and as a turbine in the other direction (reversible).
3. **Volumetric compressors**: as in other courses we have polytropic or isentropic efficiency, we can define volumetric compressors.
4. **Compressors $\rho \neq cst$** : we need to consider the axial and centrifugal systems separately because they are very different and complicated.

1.1.2 Classification of turbomachines

If the role of the machine is to extract energy from the fluid to the shaft we speak about **turboproducers** or **turbomotors** (ex: hydraulic turbines), and in the other case **turboabsorbers** or **turbogenerators**.

1.1.3 General organization of turbomachines

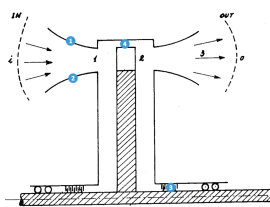


Figure 1.1

We always have a **shaft**, and on the shaft we have a **disk** or a **rotor** where the energy transformation takes place, and on this we put a **blade** (white rectangle on Figure 1.1), an element with a given geometry. The blade is situated at a distance r_H from the shaft and implies high tangential velocities. The device is closed by a **carter** and we have to be careful at the top of the blade since there can be

leakage, this is why the clearance is very small (μm). We can also have active clearance control by blowing fluid on the carter. Remark that there is an **external carter** (blue 1) and an **internal carter** (blue 2) that can constitute a convergent distributor and a divergent diffuser. These can contain non rotating parts called **vane**, we speak of **vaned convergent**, **vaned divergent** or **vaneless** nozzles. The internal carter plays the role of support and is connected to the shaft via **bearings** and **seals** (to avoid air preferring this way to reach atmospheric pressure).

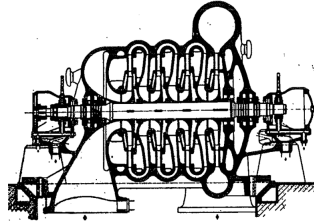


Figure 1.2

The major types of machine have an axial configuration so that the particles flows parallel to the shaft, radial configuration where flows enters horizontal and leaves vertical also exists. Most turbines or compressors are axial turbines. Turbopumps are most of the time radial, centrifugal. Several disks can be mounted on a same shaft (or several shafts), with fixed components changing the direction of the flow (multistage pump on Figure 1.2).

1.1.4 Notations

On Figure 1.1, 0 is the inlet of the distributor, 1 the inlet of the rotor, 2 outlet of the rotor, 3 outlet of the diffuser and o/s the upstream/downstream plenum. There are 3 velocity components: the absolute velocity \bar{v} , the frame tangential velocity \bar{u} and the relative velocity \bar{w} due to the rotation of fluid particles.

1.1.5 Velocity triangle

The absolute velocity respects:

$$\bar{v} = \bar{u} + \bar{w}. \quad (1.1)$$

By defining α and β the angle between \bar{u} and respectively \bar{v} and \bar{w} , we can write:

$$v \cos \alpha = u + \cos \beta \quad w^2 = u^2 + v^2 + 2uv \cos \alpha \quad (1.2)$$

The velocity triangle is the keypoint of a turbomachine, we have to play with the velocities by means of the mass flow rate \dot{m} and the machine rpm N . It is important to see that these parameters are linked to the velocity triangle, for the mass flow for example $\dot{m} = \rho u A$.

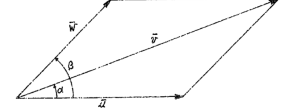


Figure 1.3

1.2 Fundamental equations of the flow

1.2.1 Equations of the flow in a fixed frame

For all developments, only **steady state** regime is considered, so that $\omega = cst$ and the flow properties are not time dependent. Moreover, boundary layers are neglected and the flow propagates in parallel slices.

Energy equation

Let's consider sections A_0 and A_1 denoting the input and output of a non interrupted flow section, for instance 0 to 1 in previous figure. The total energy equation is:

$$q = h_1 - h_0 + \frac{v_1^2 - v_0^2}{2} + g(z_1 - z_0) \quad (1.3)$$

where q is the heat exchanged with the outside [J/kg], v is the absolute velocity [m/s] and h is the enthalpy [J/kg]. In adiabatic systems $q = 0$. We see that if there is thermal, kinetic or potential energy loss, it will create heat. Be careful that this equation is not applicable around the blade.

Equation of kinetic energy

We know that kinetic and potential energy can be transformed into work in a machine. We have:

$$\frac{v_1^2 - v_0^2}{2} + g(z_1 - z_0) = - \int_{p_0}^{p_1} \nu dp - w'_f \quad (1.4)$$

where $\nu = 1/\rho$ is the specific volume [m^3/kg] and w'_f the work resulting from all friction effects [J/kg]. We see that if velocity increases/decreases, pressure decreases/increases and the friction is a loss, so "-" signs.

Global thermodynamic equation

By considering (1.4) in (1.3):

$$q + w'_f = h_1 - h_0 - \int_{p_0}^{p_1} \nu dp \quad (1.5)$$

The physical content is different, we see that in fact the losses corresponds to pressure and temperature losses.

Mass flow rate equation

The mass flow is constant over a tube:

$$\dot{m} = \rho v A = \rho_0 v_0 A_0 = \rho_1 v_1 A_1 = \frac{v_1 A_1}{\nu_1} \quad (1.6)$$

where \dot{m} [kg/s].

1.2.2 Equations of the flow in a moving frame

Now we can consider the indices 1 and 2 referring to the blade space.

Equation of kinetic energy in a relative space

He skipped the long demo page 8. The equations are the same as before, the only difference is that we replace the absolute velocity by the relative one and an additional kinetic energy term due to the rotation of the frame:

$$\frac{w_2^2 - w_1^2}{2} + g(z_2 - z_1) = - \int_{p_1}^{p_2} \nu dp - w''_f + \frac{u_2 - u_1}{2} \quad (1.7)$$

Remark that this term can play a huge role because in a centrifugal system the term is non zero while zero in axial system.

Global thermodynamic equation

The equation is exactly the same as before, except w'_f that becomes w''_f .

$$q + w''_f = h_2 - h_1 - \int_{p_1}^{p_2} \nu dp \quad (1.8)$$

Energy equation

If we combine the two previous equation we get:

$$q + \frac{u_2 - u_1}{2} = h_2 - h_1 + \frac{w_2^2 - w_1^2}{2} + g(z_2 - z_1) \quad (1.9)$$

Mass flow equation rate equation

For a section normal to the relative velocity:

$$\dot{m} = \rho w A = \rho_1 w_1 A_1 = \rho_2 w_2 A_2 \quad (1.10)$$

1.3 Fundamental equations of turbomachinery

1.3.1 Compressors

Internal losses

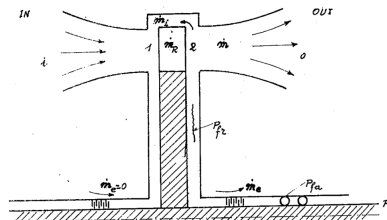


Figure 1.4

Several kind of losses are present in a compressor. First of all, friction in the distributor gives birth to losses noted w'_f . Then, the fluid go through the interblade channel where its energy increases, but a loss due to friction is present w''_f . In addition, the clearance between the blade tip and the carter is non zero and leads to back-flow leakage \dot{m}_i as the pressure upstream is lower. If we denote the mass flow rate through the blades \dot{m}_R , we have:

$$\dot{m}_R = \dot{m} + \dot{m}_i \quad (1.11)$$

Big part of the flow goes then through the diffuser, but a small part escapes from the seal to the outside \dot{m}_e . The small gap between the rotor and the internal carter is filled with part of the fluid. Even if this fluid does not contribute to the energy exchanges (stagnation), part of the power supplied to the shaft will dissipate due to fluid friction P_{fr} .

External losses

As discussed, part of the flow escapes through the seals. The upstream one is not a problem since the pressure is close to the atmospheric one, but for the downstream $\dot{m}_e \neq 0$ since the pressure is higher. This will be neglected in the study. The last losses are due to bearings and other mechanical components such as the fuel pump that we all denote in a single absorbed power P_{fa} .

Energy equation

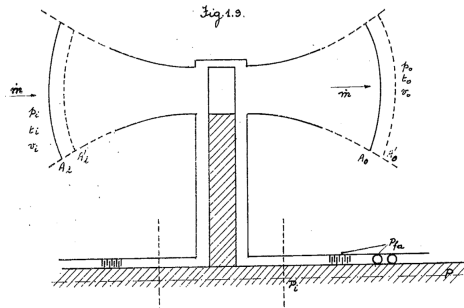


Figure 1.5

Before going through all the losses appearing in the engine, let's have a global view limiting the study region as on the figure. The total energy equation between input and output is:

$$q + W_{e \rightarrow s} = u_o - u_i + \frac{v_o^2 - v_i^2}{2} + g(z_o - z_i) \quad (1.12)$$

where we have the heat exchanged with the outside, the work from external forces to the system due to

fluid pressure $p_i\nu_i - p_o\nu_o$ and work applied on the shaft $\frac{P - P_{fa}}{\dot{m}} = \frac{P_i}{\dot{m}}$ equal to the variation of internal energy, kinetic energy and potential energy. Heat exchanges and the height difference in such engine is negligible, by introducing the enthalpy instead of internal energy and fluid pressure, we have:

$$P_i = P - P_{fa} = \dot{m} \left(h_o - h_i + \frac{v_o^2 - v_i^2}{2} \right) = \dot{m}(h_{t_o} - h_{t_i}) = \dot{m}c_p(T_{t_o} - T_{t_i}) \quad (1.13)$$

where the index t denotes the total or stagnation quantities. We conclude that the work transferred through the shaft increases the total energy of the fluid.

Equation of kinetic energy

This adapted to the work $\frac{P_i}{\dot{m}}$ gives:

$$P_i = \dot{m} \underbrace{\left(\frac{v_o^2 - v_i^2}{2} + \int_i^o \nu dp + g(z_o - z_i) \right)}_e + P_f = \dot{m}e + P_f \quad (1.14)$$

P_f is the internal friction loss with the active as well as the non-active fluid and e is the energy transferred to the fluid.

A first distribution of the power - efficiencies

The figure summarizes all the above equations, for the efficiency we have $\dot{m}e$ at the end and we inject P so:

$$\eta_g = \frac{\dot{m}e}{P} = \frac{\dot{m}e}{P_i P} = \eta_i \eta_m \quad (1.15)$$

that we rewrite as internal efficiency and external mechanical efficiency.

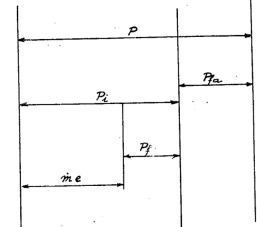


Figure 1.6

Energy transfer to the rotor

The only new equation we have is the **Euler-Rateau equation**. The energy given to the flow in a pump is linked to the energy provided to the shaft. We have to consider the kinetic moment (moment of the quantity of movement) related to the shaft:

$$\frac{d}{dt} \sum M_{axe}(m\bar{v}) = \sum M_{axe}\bar{F}_e \quad (1.16)$$

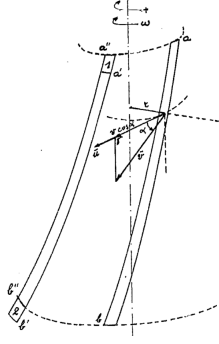


Figure 1.7

The variation of the kinetic moment of the rotor is zero since the rotation speed is constant. For a fluid element with mass m and at a distance r of the shaft, the velocity \bar{v} is composed of a component // to the shaft, radial component and tangential component on the rotor. Only the tangential component delivers a moment:

$$M_{axe}(m\bar{v}) = mrv \cos \alpha \quad (1.17)$$

and since the flow is permanent, after a time dt very small, if the mass flow is constant:

Figure 1.7

$$\sum_{b'b''} mrv \cos \alpha - \sum_{a'a''} mrv \cos \alpha = m'(r_2 v_2 \cos \alpha_2 - r_1 v_1 \cos \alpha_1) = m'(r_2 v_{2u} - r_1 v_{1u}) \quad (1.18)$$

Accepting $r_2 v_{2u} - r_1 v_{1u} = cst$ for all channels we get:

$$\frac{d}{dt} \sum M_{axe}(m\bar{v}) = \frac{d}{dt} [(r_2 v_{2u} - r_1 v_{1u}) \sum m'] = \dot{m}_R(r_2 v_{2u} - r_1 v_{1u}) \quad (1.19)$$

For the right hand side of (1.16), the weight of the wheel, the weight of the fluid, the pressure at inlet, at outlet and at side walls are null due to symmetry. Only the **driving torque** applied on the shaft M_i and the **resistive torque** $-M_{fr}$ due to friction between the wheel and the non-active fluid are present, so that we finally get:

$$\dot{m}_R(r_2 v_{2u} - r_1 v_{1u}) = M_i - M_{fr} \quad (1.20)$$

And if we multiply by ω :

Equation of Euler-Rateau

$$P_i - P_{fr} = P - P_{fa} - P_{fr} = P_R = \dot{m}_R(u_2 v_{2u} - u_1 v_{1u}) = \dot{m}_R \Delta(uv_u) \quad (1.21)$$

This equation tells that in order to be transferred to the mass flow rate \dot{m}_R , the power at the rotor shaft P_R must show an increase of the quantity uv_u which is directly related to the velocity triangle.

As $w^2 = v^2 + u^2 - 2uv_u$, one can also write:

$$P_R = \dot{m}_R \left(\frac{v_2^2 - v_1^2}{2} + \frac{u_2^2 - u_1^2}{2} - \frac{w_2^2 - w_1^2}{2} \right) \quad (1.22)$$

Energy generated by the rotor

Remember (1.7) and replace this in (1.22), we get:

$$P_R = \dot{m}_R \underbrace{\left(\frac{v_2^2 - v_1^2}{2} + \int_{p_1}^{p_2} \nu dp + g(z_2 - z_1) \right)}_{e_R} + \dot{m}_R w_f'' \quad (1.23)$$

where e_R is the energy transferred to the fluid through the channels on the rotor between section 1 and 2 on the common figure. $\dot{m}_R w_f'' = P_f''$ being the power absorbed by friction effects, we get:

$$P_R = \dot{m}_R e_R + P_f'' \quad (\text{and } P_R = \dot{m}(h_{t_2} - h_{t_1})) \quad (1.24)$$

And we get thus 4 different expression for P_R , where the last expression was given in lecture.

1.3.2 Detailed power distribution

The different losses can be depicted thanks to the previous equation:

$$P_i = P - P_{fa} \quad P_R = P_i - P_{fr} \quad \dot{m}_R e_R = P_R - P_f'' \quad \dot{m}_R = \dot{m} + \dot{m}_i \quad (1.25)$$

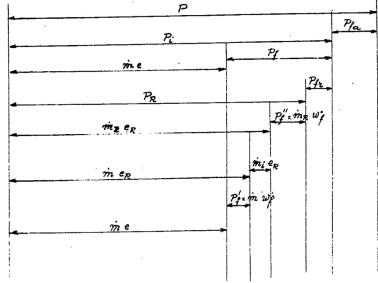


Figure 1.8

where we clearly see the mechanical losses, the loss due to stationary fluid, the loss at the rotor and the back flow. To this we have to add the loss at the diffuser and distributor which we wrote as:

$$P_f' = \dot{m} w_f' \quad (1.26)$$

On the figure, we first see the loss due to mechanical components giving P_i , then the fluid losses composed of stationary fluid losses giving P_R , then rotor channels loss giving $\dot{m}_R e_R$, but we have the back flow loss $\dot{m}_i e_R$ giving $\dot{m}_e R$ and the last venturi losses that gives the output power $\dot{m} e$ plus all the losses.

1.4 Turbines

Description

The equations are in fact the same except that we have to adapt the signs and indexes to the working principle since the energy is flowing from the fluid to the shaft. As before, there is a clearance flow \dot{m}_i such that:

$$\dot{m} = \dot{m}_R + \dot{m}_i \quad (1.27)$$

The losses due to mechanical components P_{fa} and the leakage flows \dot{m}_e (negligible), the energy losses in non rotating (w_f') and rotating (w_f'') frame and the loss due to non-active fluid P_{fr} are present. The useful power P_u replaces the P we had before.

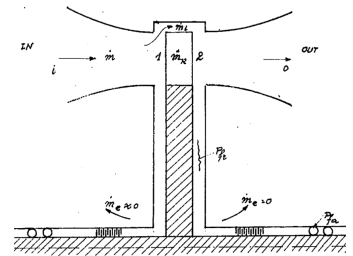


Figure 1.9

Energy equation

It is the same as before except that the indexes are inverted and the useful power is $P_u = P_i - P_{fa}$:

$$P_i = P_u + P_{fa} = \dot{m}(h_{t_i} - h_{t_o}) \quad (1.28)$$

Equation of kinetic energy

$$P_i = \dot{m} \underbrace{\left(\frac{v_i^2 - v_o^2}{2} + \int_{p_o}^{p_i} \nu dp + g(z_i - z_o) \right)}_e - P_f = \dot{m} e - P_f \quad (1.29)$$

First distribution of the power

The efficiencies are inverted:

$$\eta_g = \frac{P_u}{\dot{m}e} = \frac{P_u}{P_i} \frac{P_i}{\dot{m}e} = \eta_m \eta_i \quad (1.30)$$

On Figure 1.10 is represented a first plot of the different powers, remark that it is similar to what we had, only the fluid losses comes before the mechanical losses. The fluid losses are the same as before.

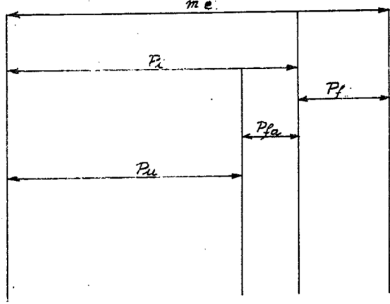


Figure 1.10

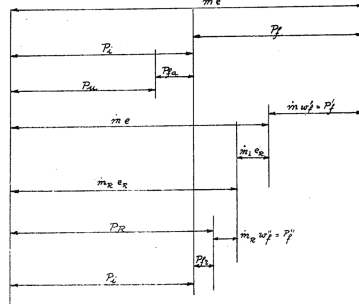


Figure 1.11

Equation of Euler-Rateau

We can rewrite P_R as the power transferred to the rotor from the fluid \dot{m}_R :

$$P_R = P_i + P_{fr} = \dot{m}_R (u_1 v_1 \cos \alpha_1 - u_2 v_2 \cos \alpha_2) \quad (1.31)$$

Energy absorbed by the rotor

As before, combining the above equation and the equation for rotating frame we get:

$$P_R = \dot{m}_R e_R - P_f'' \quad (1.32)$$

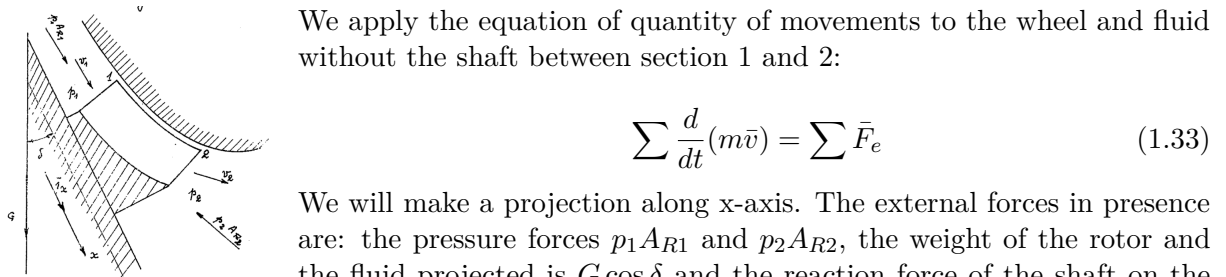
1.5 Axial thrust and disc friction

1.5.1 Definition

Since the turbomachinery is used to increase the energy of the fluid or extract energy, the pressure at the two sides of the rotor is different. This leads to an axial force and we need **thrust bearings** to avoid the shaft to slip.

1.5.2 Equation of the axial thrust

We apply the equation of quantity of movements to the wheel and fluid without the shaft between section 1 and 2:



We will make a projection along x-axis. The external forces in presence are: the pressure forces $p_1 A_{R1}$ and $p_2 A_{R2}$, the weight of the rotor and the fluid projected is $G \cos \delta$ and the reaction force of the shaft on the

Figure 1.12

rotor with projection F_{ax} so $-F_{ax}$ as seen by the rotor (projection of moments is null). The equation of quantity of movement becomes:

$$\begin{aligned} \dot{m}_R (v_{2ax} - v_{1ax}) &= p_1 A_{R1} - p_2 A_{R2} + F_{ax} + G \cos \delta \\ \Leftrightarrow F_{ax} &= \dot{m}_R dt(v_{2ax} - v_{1ax}) + P_2 A_{R2} - P_1 A_{R1} - G \cos \delta \end{aligned} \quad (1.34)$$

1.5.3 Friction of the disc

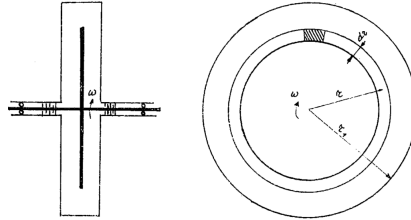


Figure 1.13

As mentioned before, there is friction between the disc and the non-active fluid. It is obvious that the friction torque will increase with the radius (more surface), the rpm (u) and the volumetric mass of the fluid. Considering an elementary surface $2\pi r dr$, we find experimentally for the elementary friction force and torque:

$$dF_{fr} = K\rho u^2 2\pi r dr \quad dC_{fr} = 2K\rho 2\pi r^2 dr u^2 \quad (1.35)$$

the 2 appears by considering the 2 sides of the disc. We integrate from internal radius r to the external one r_1 and multiply by ω to have powers (neglect r^5 compared to r_1^5):

$$C_{fr} = K\rho\omega^2 r_1^5 \quad \Rightarrow P_{fr} = K\rho\omega^3 r_1^5 \quad (1.36)$$

Remark that one could think that we will have enormous values for ω^3 , but be aware that if ω increases, the mechanical stresses on the device increases and force to reduce the r_1 . This is why the friction is finite. If the side walls are very smooth, the coefficient K is related to the Reynolds number:

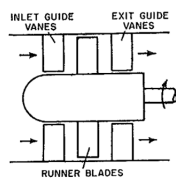
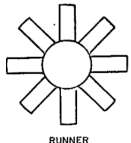
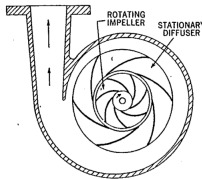
$$Re = \frac{\rho\omega r_1^2}{\mu} \quad (1.37)$$

Chapter 2

Centrifugal pumps

2.1 Generalities

2.1.1 Description - Type of turbopump



The task of the turbopump is to transfer

Figure 2.1

Figure 2.2

energy to a liquid. Above we can see a centrifugal and an axial turbopump. Between these two extremes, we can have a variety of types depending on the requirements. Each turbopump is composed of one or several wheels that can be mounted in parallel (increase mass flow rate) or in series (higher energy transfer), see Figure 1.2.

2.1.2 Installation of a turbopump

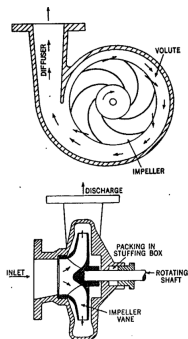


Figure 2.3

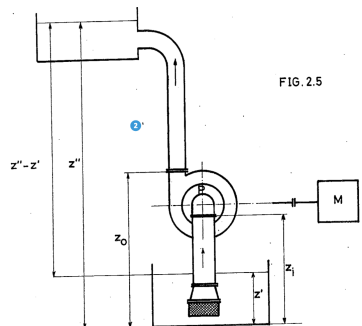


Figure 2.4

that the flow enters at the middle in the rotating blade and is projected into the volute. This last has a growing section from the beginning to the end as the mass flow increases. The turbopump is commonly used to transfer liquid from a downstream reservoir to an upstream reservoir situated higher. We have to be careful to avoid cavitation (evaporation of the fluid due to too low pressures) and we also have a control valve at the suction section to always have a contact blade-fluid.

2.1.3 Energy developed by the turbopump - flow rate

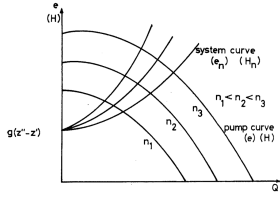


Figure 2.5

$$e = \frac{v_o^2 - v_i^2}{2} + \int_{p_i}^{p_o} \nu dp + g(h_o - h_i) = \frac{v_o^2 - v_i^2}{2} + \frac{p_o - p_i}{\rho} + g(h_o - h_i) \quad (2.1)$$

The velocity is low in order to limit the head losses and thus the pressure term is the highest (height change in a compressor is low too). The energy delivered by the pump to the fluid can be rewritten in terms of the volumetric flow rate Q [m^3/s]:

$$e_p = \frac{p_a - p_i}{\rho} - \frac{p_a - p_o}{\rho} + \frac{A_i^2 - A_o^2}{2A_i A_o} Q^2 + g(z_o - z_i) \quad (2.2)$$

2.1.4 Useful power or hydraulic power

The power transferred from the input of the pump until the exit and the global efficiency of the pump are:

$$P_h = \dot{m}e = \rho Q e \quad [W] \quad \eta = \frac{\rho Q e}{P_m} \quad (2.3)$$

where P_m is the mechanical power to drive the pump.

2.1.5 Working point of a turbopump

Consider Figure 2.4 and let's apply Bernouilli equation (kinetic energy equation) between z' and z_i then z_o and z'' :

$$\frac{v_i^2 - v'^2}{2} + g(z_i - z') = -\frac{p_i - p'}{\rho} - w'_{fa} \frac{v''^2 - v_o^2}{2} + g(z'' - z_o) = -\frac{p'' - p_o}{\rho} - w'_{fr} \quad (2.4)$$

One can make the sum of the two expression and regroup the terms of the reservoirs in a new **energy requested by the circuit e_n** . If we consider large reservoirs $v'' \approx v'$ and $p'' \approx p' \approx p_a$, we have:

$$e_n = g(z'' - z') + \underbrace{w'_{fa} + w'_{fr}}_{w'_f} \Rightarrow e_p = e_n \quad (2.5)$$

This is always valid in **steady state**.

2.1.6 Characteristic of the hydraulic circuit

The system curves on Figure 2.5 plot e_n which depends on the height difference and the mass flow rate (because $w'_f \propto v^2$ of the flow) and depends thus on the square of the volumetric mass flow rate. This is why we have a parabolic shape, the slope depends on the head loss coefficient K . If we have a valve, the closer the valve, the higher the slope.

2.1.7 Performance curve of a pump

Similar curves can be established for the e, Q relations at different rpm. With a control valve at the exit, and by fixing the rpm of the engine, we can find them and are plotted on Figure 2.5.

2.1.8 Working regimes

Practical analysis shows that if two of the three parameters e, Q, n are fixed, the working point too: $f(e, Q, n) = 0$

2.1.9 Practical units

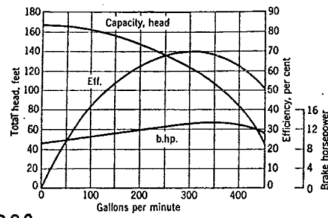


FIG.2.8.

Figure 2.6

Here we express the energy in J/kg but we know that it is also $g\Delta z$ in [m]. Thus we will use instead of e , $H = e/g$ [m]. The energy transferred to the fluid is often called the **height** of the **head**. For example $H = 10$ m means that we transfer energy such that we increase z of 10 m. As last remark, be aware that efficiency curves are provided by the manufacturer and the pump has to be chosen specifically to the circuit where it should operate to get the maximum efficiency.

2.2 The centrifugal pump

2.2.1 Organization of a centrifugal pump

We have an inlet distributor D charged of guiding the fluid towards the entrance 1 of the rotor R or also called **impeller**. The rotor is made of one or two disks on which are mounted the blades beginning at a certain external radius r_1 and finishing at r_2 . A fixed diffuser d composed of 2 parallel discs surrounding the rotor, connected with vanes surrounds the exit of the blades, sometimes it is not used. A **volute** or **collector** c with increasing volume directs the flow to the exit section of the machine.

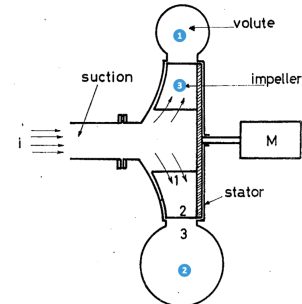


Figure 2.7

2.2.2 The distributor

If there is no vane in the distributor, the flow penetrates in the rotor axially since we assume no fluid particle to rotate before entering in the rotor, and becomes radial symmetrically at entrance 1. If there is vane, the direction of the flow is imposed by the vanes but we take the first case here. The equation of kinetic energy applied between i and 1 when neglecting the height difference is:

$$\frac{v_i^2 - v_1^2}{2} + \frac{p_i - p_1}{\rho} = w'_{fD} \quad (2.6)$$

where w'_{fD} represents the pressure losses in the distributor, proportional to the square of Q and thus to v_1^2 : $w'_{fD} = K_D \frac{v_1^2}{2}$ where $K_D \approx 5.10^{-3}$

2.2.3 The rotor

The impeller starts at r_1 and finish at r_2 , the section of the rotor at these levels are:

$$A_1 = 2\pi r_1 b_1 e_1 \quad A_1 = 2\pi r_2 b_2 e_2 \quad (2.7)$$

where e_1, e_2 are blockage coefficients taking into account the decrease in area due to the thickness of the impeller.

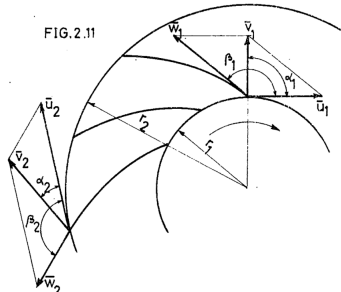


Figure 2.8

The rotor and impeller velocity triangles are represented on the figure. v_1 is known by the previous discussion and is purely radial and u_1 can be computed:

$$v_1 = \frac{Q_R}{2\pi r_1 b_1 e_1} \quad u_1 = r_1 \omega_1 = \frac{2\pi n}{60} r_1 \quad \alpha_1 = 90^\circ \quad (2.8)$$

The missing components of the velocity triangles are w_1 and β_1 and can be retrieved by construction. In addition we make an assumption for β_1 (fluid angle) which must be equal to $\bar{\beta}_1$ (solid angle), this is imposed by the design to avoid collision or separation. Indeed, the pump is designed to work with a certain Q_R and a certain n , if this changes, shocks and separation can occur, leading to losses. Same considered for β_2 , $u_2 = r_2 \omega$ and this time the radial velocity is the projection of w_2 :

$$u_2 = r_2 \omega_2 \quad w_2 \sin \beta_2 = \frac{Q_R}{2\pi r_2 b_2 e_2} \quad (2.9)$$

β_2 is chosen larger than 90° in order to make v_2 small and thus limit the diffuser size (limit the losses, β_2 between 145° and 165°). We are now able to retrieve v_2 and w_2 .

2.2.4 Number and shape of the blades

The number of blades determine the volume available to the flow and the guidance. The more we have blades, the more the fluid is guided but the more we have pressure losses. The designer must make a trade-off, generally there are 6 to 12 blades. The profile of the blades must be so that the angles $\beta_1 = \bar{\beta}_1$ and $\beta_2 = \bar{\beta}_2$ are respected.

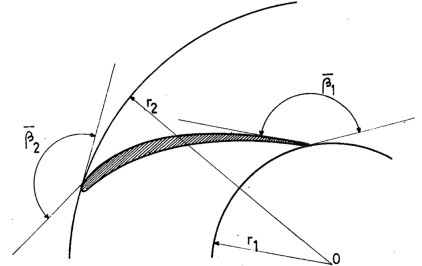


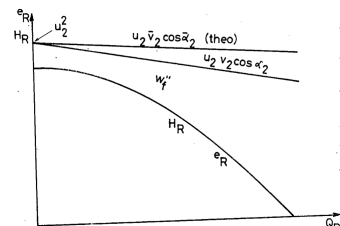
Figure 2.9

If the blades are made of two surfaces, one active and one non-active as represented on the figure, if the two surfaces makes an angle too large at the entrance, it is impossible that β_1 is tangent to both and lead to shocks. At the exit, since there is a pressure gradient between active and non active sides, the β_2 is "sucked" by the non-active part where the pressure is lower.

2.2.5 Head of Euler of the rotor

Using Euler-Rateau and power distribution, we have:

$$P_R = \dot{m}_R (u_2 v_{2u} - u_1 v_{1u}) = \dot{m}_R e_R + \dot{m}_R w_f'' \Rightarrow e_R = u_2 v_{2u} - u_1 v_{1u} - w_f'' \quad (2.10)$$



as we have seen, $\alpha_1 = 90^\circ \Rightarrow v_{1u} = 0$ and $e_R = u_2 v_{2u} - w_f''$. The term $u_2 v_{2u}$ is called the **energy of Euler** and is the theoretical energy that the rotor transfers to the fluid. The **head of Euler** is $\frac{u_2 v_{2u}}{g}$. Lets show that this energy is function of $Q_R, N, \bar{\beta}_1$ and $\bar{\beta}_2$ using the velocity triangle relation:

Figure 2.10

$$\mathbf{u}_2 v_2 \cos \alpha 2 = \mathbf{u}_2 (u_2 + w_2 \cos \bar{\beta}_2) \Rightarrow e_r = u_2^2 + \frac{Q_R}{2\pi r_2 e_2 b_2 \tan \bar{\beta}_2} \quad (2.11)$$

where we used (2.9). We see that as $\bar{\beta}_2 > 90^\circ$ in practice, we have a linearly decreasing function. We still don't have the characteristics since we are underestimating the angles deviation, the number of blades and the fluid losses.

2.2.6 Losses in the rotor due to friction

He skipped the previous section. The term w_f'' regroups the different losses that occurs in the rotor and can be separated in:

- the losses due to the development of the boundary layer in the channel sidewalls and $\propto Q_R^2$:

$$k_1 Q_R^2 = K_R \frac{w_1^2}{2} \quad K_R \approx 0.025 \quad (2.12)$$

- a second loss due to the shocks and separation of the boundary layer each time w_2 is not tangent to the blade. Looking to the situation on Figure 2.11, we find experimentally that these losses are $\propto (\Delta w)^2$ that is $\propto v_1$ that is $\propto Q_R - Q_{RD}$ where Q_{RD} is the flow rate in design conditions $\beta_1 = \bar{\beta}_1$:

$$Q_R = 2\pi r_1 b_1 e_1 v_1 \quad Q_{RD} = 2\pi r_1 b_1 e_1 v_{1D} \quad (2.13)$$

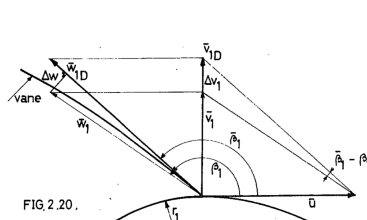


Figure 2.11

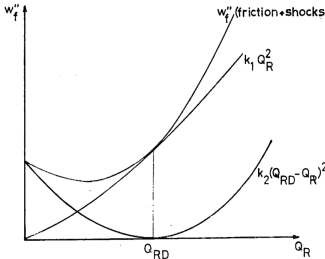


Figure 2.12

The sum is represented on Figure 2.12 and we see that even at low Q_R w_f'' is high, this is due to the second loss.

2.2.7 Loss due to the internal leak flow

We already know what it is, it goes from 1 for large pumps to 10% of \dot{m}_R for small pumps. This is due to the fact that the clearance cannot be reduced under an absolute size and the seals in large machines cannot be more efficient than in small machines. The power loss is:

$$\dot{m}_i e_R = (0.01 \text{ to } 0.1) \dot{m}_R e_R \quad [W] \quad (2.14)$$

2.2.8 Friction of the disc on the non-active fluid

Per side of the disc, it can be estimated as:

$$P_{fr} = 1.21 \cdot 10^{-3} u_2^3 D_2^2 \quad [ch] \quad (2.15)$$

2.2.9 The diffuser

Energy transformation in the diffuser

The velocity v_2 at the exit of the pump is generally too high for some applications, the diffuser converts part of the kinetic energy into pressure energy. There exists 4 types of diffuser: straight parallel sidewalls or inclined, and for each we can have vaneless or vaneless. The kinetic energy equation in a fixed frame with $z_3 - z_2 = 0$ is:

$$\frac{p_3 - p_2}{\rho} = -\frac{v_3^2 - v_2^2}{2} - w'_{fd} \quad (2.16)$$

where $w'_{fd} \approx 0.02 - 0.03v_2^2/2$ [J/kg]. We see that kinetic energy gives pressure and loss.

The vaneless diffuser with flanges

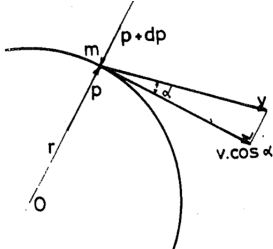


Figure 2.13

The common architecture of the diffuser is composed of two circular flanges put around and in the continuity of the exhaust of the rotor. Let's apply the equation of the kinetic moment to a fluid element of mass m and at a radius r :

$$\frac{d}{dt} M_{axis}(m\bar{v}) = M_{axis} \bar{F}_e \quad (2.17)$$

The situation is represented on Figure 2.13, the flow in the diffuser is axisymmetric. If one neglect the weight of the particles, the external forces moment is null since the pressure is radial. All particles are facing the same pressure for symmetrical reasons and have thus the same trajectory. We have:

$$\frac{d}{dt}(mvr \cos \alpha) = 0 \quad \Leftrightarrow mvr \cos \alpha = rv_u = cst \quad (2.18)$$

This is valid for a non-rotational flow. On the other hand we have the mass flow rate:

$$2\pi rb \sin \alpha = cst \quad \Rightarrow b \tan \alpha = cst \quad (2.19)$$

If the flanges are parallel $b = cst$ and thus $\alpha = cst$, this gives a logarithmic spiral for the particles trajectory. The only way to make v_3 decrease is to have larger r_3 :

$$2\pi r_2 b_2 v_2 \sin \alpha_2 = 2\pi r_3 b_3 v_3 \sin \alpha_3 \quad \Rightarrow v_3 = v_2 \frac{r_2}{r_3} \quad (2.20)$$

Another way is to have variable b . In (2.19) this would mean that α decreases. We have thus:

$$2\pi r_2 b_2 v_2 \sin \alpha_2 = 2\pi r_3 b_3 v_3 \sin \alpha_3 \quad \Rightarrow v_3 = v_2 \frac{r_2 b_2 \sin \alpha_2}{r_3 b_3 \sin \alpha_3} = v_2 \frac{r_2 \cos \alpha_2}{r_3 \cos \alpha_3} \quad (2.21)$$

Since $\cos \alpha_3 > \cos \alpha_2$, v_3 will be lower. The divergence angle is limited to 6-7° because of separation (have to look for another method).

The diffuser with blades

With the previous discussion, if v_2 increases we still have to increase r_3 . Another method to avoid this, is the use of vanes between the flanges. Their job is to guide the fluid particle so that α increases:

$$2\pi r_2 b_2 v_2 \sin \alpha_2 = e_3 2\pi r_3 b_3 v_3 \sin \alpha_3 \quad \Rightarrow \frac{r_3}{r_2} = \frac{1}{e_3} \frac{v_2 \sin \alpha_2}{v_3 \sin \alpha_3} \quad (2.22)$$

where e_3 is the filling coefficient taking into account the presence of the vanes. We see that for higher α_3 , we can take lower r_3 . But blade means friction and thus shock.

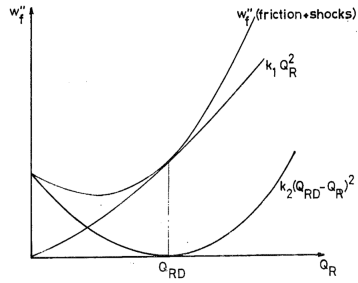


Figure 2.14

To avoid this the entrance of the diffuser should be 1 or 2 mm larger and the vanes should be tangent to the flow, depending on Q and N . The design is thus made in order to be tangent for a certain couple N_D, Q_D called design conditions. In off-design conditions, shocks and separation occur. There is a small gap between vanes and the rotor blades to limit the noise produced by turbulences. Due to the shocks and separation, w'' is never equal to zero and rather large for small Q . In conclusion, the vaned diffuser gives smaller dimensions, but lead to considerable losses when far from the working point and it is maybe

2.2.10 The volute or collector

Its job is to collect the flow coming out of the diffuser or the rotor, it's section increases from the beginning to the end, the flow in radial section is non uniform and respects:

$$v_y r = v_{y3} r_3 = cst \quad (2.23)$$

and the losses in the diffuser and volute are estimated to (0.02 and 0.03) $\frac{v^2}{2}$ [J/kg].

2.2.11 Characteristic curves of a centrifugal pump

We are now able to understand the shape of the characteristic curve on Figure 2.10 since the losses w_f'' have a parabolic shape. To deduce the curve in function of the flow Q , we still have to consider the internal leak flow $Q = Q_R - Q_i$ and the w'_{fD} and w'_{fd} that are function of Q^2 and $(Q - Q_D)^2$ when the diffuser is vaned. We can make these curves for different rpm it goes up and right, we will see how to plot them without experiment, we only have to measure for one rpm.

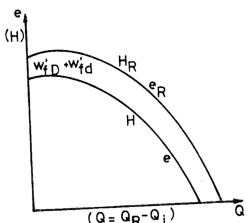


Figure 2.15

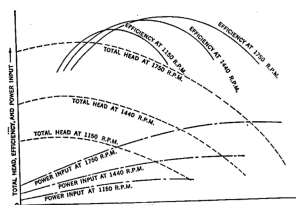


Figure 2.16

2.3 Performance curves of centrifugal pumps non-dimensional analysis

2.3.1 Theory of Vachy-Buckingham

Consider a machine characterized by some physical variables containing q fundamental parameters. It is possible to choose p independent variables and to build $p - q$ independent non-dimensional variables. Any other dimensionless combination of these variables will be function of the independent reduced variables.

2.3.2 Application to turbopumps

The variables differentiating geometrically equivalent pumps working points are: r [L], n [T^{-1}], \dot{m} [MT^{-1}], ρ [ML^{-3}] and μ [$ML^{-1}T^{-1}$]. We can limit the physical variables to 4 parameters by noticing that $u = r \frac{2\pi n}{60}$ and that μ is in Re number already non-dimensional and 3 fundamental variables. The non-dimensional variable can be found as follows:

$$\begin{aligned}\pi &= r^x u^y \dot{m}^z \rho^w \Rightarrow \pi = (L)^x (LT^{-1})^y (MT^{-1})^z (ML^{-3})^w = M^0 L^0 T^0 \\ x + y - 3w &= 0 \quad -y - z = 0 \quad z + w = 0\end{aligned}\quad (2.24)$$

We have a system of 3 equations with 4 variables, we will fix $z = 1$ to have \dot{m} in the expression, that gives $y = -1, w = -1, x = -2$, and the reduced variable is:

$$\frac{\dot{m}}{\rho u r^2} = \frac{Q}{u r^2} \Rightarrow \frac{Q}{u r^2} \cdot \frac{\dot{e}}{u^2} \cdot \eta_g \cdot \frac{\dot{P}}{\rho u^3 r^2} \quad (2.25)$$

2.3.3 Performance curves of a type of pumps

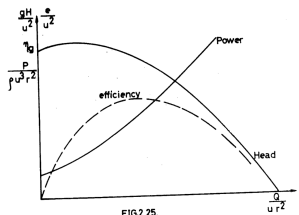


Figure 2.17

For a family of pumps with same r, ρ and u we can plot the non-dimensional $\frac{gH}{u^2}, \eta_g, \frac{P}{\rho u^3 r^2}$ in function of the non dimensional $\frac{Q}{\rho u r^2}$. If two of the parameters are known, the third is known since:

$$\frac{P}{\rho u^3 r^2} = \frac{P}{\dot{m} e} \frac{\dot{m}}{\rho u r^2} \frac{e}{u^2} = \frac{1}{\eta_g} \frac{Q}{u r^2} \frac{gH}{u^2} \quad (2.26)$$

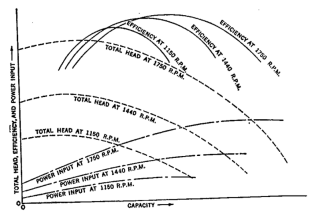


Figure 2.18

2.3.5 Stability of a turbopump

Stability of the motor + pump assembly

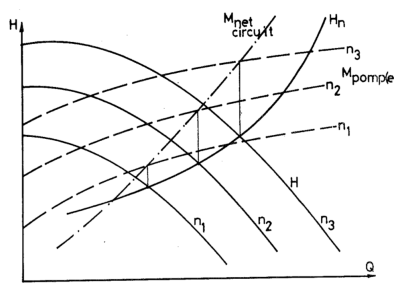


Figure 2.19

This is based on the driving torque of the motor and resistive torque of the pump. These can be found considering the characteristic curve of a pump in a fixed network. For what concerns the torque curve of the pump, one just has to divide the H curve by the rpm and will get a torque curve for every rpm. For the resistive torque, determine the intersection of $H_{network}$ and H_{pump} and make the projection on the pump torque for every rpm. We find a positive slope curve.

Stability of the pump on the circuit

The second stability problem is the problem of the pump in the circuit. Consider the figure illustrating a water tower without losses inducing a horizontal network characteristic, (b) has a small design mass flow rate and the other (c) large. The small one has in fact the same curve as the second but the maximum is shifted on the y-axis.

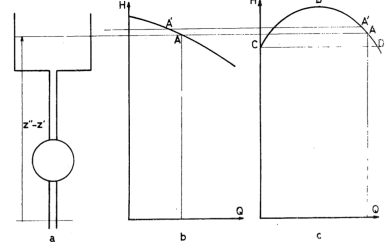


Figure 2.20

Now, imagine a town to supply with a water tower. At a given moment we have a certain amount of users, and we are at point A. If now there are using less and less of water, the level of water is increasing so that more power is requested from the pump. The two configuration are good in the sense where the increase of the level makes the flow reduce. If now the level goes higher and higher until reaching the maximum of the curve, the pump stops, there is no intersection on the curve. The configuration (b) is ok because the level drops the pump is used normally.

But for configuration (c), when the pump stops, we go directly to point C and when the level drops, the pump will be functional only when the level reaches C and has a jump to point D. The problem is that the flow is maximal and the level goes rapidly up such that we have a cycle ABCD. This is called **surge mode**. This is a low frequency loop because it requires time to go from D to B ($\approx 1 \text{ Hz}$). In conclusion, the (b) is very good for stability but not for performance and the contrary for the other. So we want to combine the two. We put a c pump on the network that is always used and we have in parallel another pump b that will be used at high levels.

2.3.6 Pump cavitation

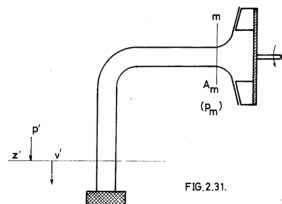


Figure 2.21

When the pump is placed above the free fluid level, the intrance pressure should be less than the atmospheric pressure to allow suction. We can define the minimum section as the end of the distributor. When Q increases this will be the place of high velocities and thus low pressures. When the pressure is lower than the saturation pressure, gas bubbles or vapor pockets will be formed. There are problems due to the gas dissolved in the fluid:

- reduction of the flow rate due to narrowing of the fluid section;
- noise characteristic of the phenomenon and changing with the intensity of the cavitation;
- degradation of the blades due to the interaction with bubbles, they produce a locally concentrated stress, erosion and corrosion of the metal of the blades.

The pressure at the minimum section can be found by using the kinetic energy equation between free level and minimum section, expressing the losses as kQ^2 and replacing the velocity by $v_m = Q/A_m$:

$$\frac{v_m^2 - 0}{2} + g(z_m - z') + \frac{p_m - p_a}{\rho} = -kQ^2 \quad \Rightarrow p_m = p_a - g\rho(z_m - z') - \rho \left(k + \frac{1}{2A_m^2} \right) Q^2 \quad (2.27)$$

Using this formula we can see that increase of Q makes p_m smaller, same for decrease of A_m , increase of k and higher level differences. The gas to liquid ratio is also important (ability to liberate gas into the liquid). The saturation pressure is changing with temperature. What we

can do to avoid cavitation is to place the pump at the same level as the free level or below, and avoid all the friction before the entrance such as additional valves or pipe turns,

We can conclude by stating that a modification in the circuit can have important consequences on the efficiency of a pump, always check!

NSPH

In order to make rise a column of fluid, underpressure is needed for suction. If this underpressure is lower than the saturation pressure of the fluid, cavitation will take place. If the water head to be sucked is too important to be elevated without cavitation, one has to use several pumps. The maximum possible underpressure before cavitation is called the available NPSH (Net Positive Suction Head). This is related to the water head aspiration, there is also one related to the pump flow rate since we need an extra underpressure to give a certain more or less high flow rate called requested NPSH:

$$NPSH_{avail} = H_e - \frac{p_s}{\rho g} \quad NPSH_{avail} > NPSH_{req} \text{ to avoid cavitation} \quad (2.28)$$

2.4 The network and its characteristic curve

2.4.1 Simple circuit

By simple circuit we mean the one composed by two reservoirs the pipes and one turbopump. If we apply the kinetic energy equation between ' and i and between o and " we can combine them and get:

$$\frac{v''^2 - v'^2}{2g} + \frac{p'' - p'}{\rho g} + (z'' - z') + \frac{\sum w_f}{g} = \frac{v_o^2 - v_i^2}{2g} + \frac{p_o - p_i}{\rho g} + (z_o - z_i) \quad H_n = H \quad (2.29)$$

H_n is the characteristic of the circuit. In a simple configuration as in Figure 2.4 we have $v'' = v' \approx 0$ and $p'' = p' = p_a$ such that:

$$H_n = (z'' - z') + \frac{\sum w_f}{g} \quad (2.30)$$

but in some applications we cannot neglect these terms so that we have 2 terms independent of Q^2 and two dependent and thus the actual characteristic $H_n(Q)$ is the increasing part of a parabol beginning at ordinate $z'' - z' + \frac{p'' - p'}{\rho g}$.

2.4.2 Calculation of the characteristic curve of a circuit

Losses in the circuit

We consider non incrusted circular pipes for turbulent pipes:

$$Re = \frac{vD}{\nu} > 2500 \quad (2.31)$$

where ν is the kinematic viscosity. There will be losses in straight pipes, accessories and shape modifications.

Regular pressure losses (in straight pipes)

They are $\propto L, Q(\nu), \nu$ and inversely $\propto D^2$.

Singular losses (in all accessories)

They can be replaced by equivalent straight pipe losses thanks to coefficients listed in a table that one must multiply by the diameter in cm to get m. Each accessory has its own coefficient.

Losses due to abrupt shape modifications

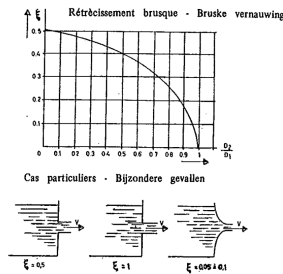


Figure 2.22

They are computed in meter using the formula:

$$\zeta \frac{v^2}{2g} \quad (2.32)$$

where v is the downward velocity in case of an opening of the section and backward in the case of a restriction. In the case of a section increase:

$$\zeta = \left(\frac{D_{aval}^2}{D_{amont}^2} - 1 \right) \quad (2.33)$$

In the case of a restriction the value is computed using the graph. An example of computation is made at page 56, a remark: in case of rough pipes more rigorous computations must be made.

Complex circuits

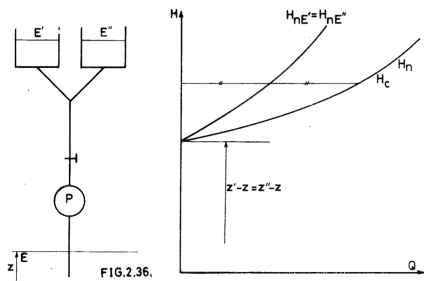


FIG.2.36.

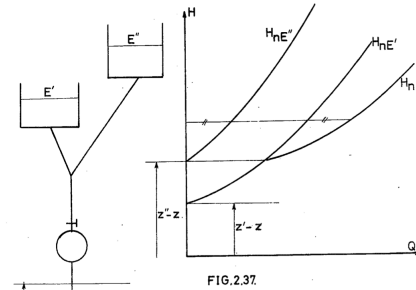


FIG.2.37.

Figure 2.23

Figure 2.24

In the case of complex circuits like the two above, one has just to consider the two characteristics, which are superimposed in the first case since the water head is the same and where they are different in the second case because of the height difference (start on y-axis). In the first case, once the pump is able to deliver to one of the reservoir it is also able to deliver to the other and thus we need a larger flow rate. This manifests by doubling the x-axis. In the second case, when the height is between z' and z'' only the lower one is filled, and once we arrive at z'' the combination is made as the first case.

2.5 Selection of a pump of a pump type

2.5.1 Users of pumps

We take the point of view of the process engineer and not the designer, so we select an existing pump fitting at best the need in H and Q . The speed is normally fixed by the driving motor, variable speed could be useful to select the region of maximum efficiency for a working region

but is more expensive. A high rotation speed makes the device more compact and cheaper. We need thus to fix the circuit on which the pump will be used, the desired Q_D , the nature of the fluid ρ and the rpm N .

2.5.2 General case

For a same family of pumps, it is possible to reduce the performance curves in a single one as seen previously with non-dimensional numbers at certain rpm:

$$\frac{W_m}{\rho u^3 r^2}, \frac{e}{u^2}, \frac{gH}{u^2} \quad \eta_g \quad \text{in } f\left(\frac{Q}{ur^2}\right) \quad (2.34)$$

2.5.3 Choice of the pump type

We can plot $\left(\frac{e}{u^2}\right)^{\frac{3}{2}}$ in function of $\frac{Q}{ur^2}$ we can plot the performance curve of each family on the same graph and can target the maximum efficiency region on each curve. Let's define the angle:

$$\tan \psi = \frac{\left(\frac{e}{u^2}\right)^{\frac{3}{2}}}{\frac{Q}{ur^2}} = \frac{(gH)^{3/2} r^2}{Qu^2} = \left(\frac{60}{2\pi}\right)^2 \frac{(gH)^{3/2}}{Qn^2} \quad (2.35)$$

where we used the relation $u = \frac{2\pi n}{60}r$ for the last expression. By replacing n, Q, H by the desired ones, we can find a ψ_D that one draws on the figure and select the pump that intersects the nearest to the maximum efficiency region (here 1).

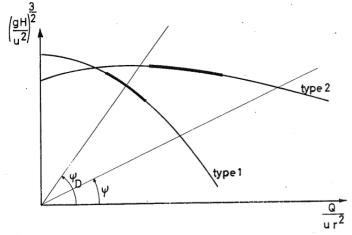


Figure 2.25

2.5.4 Choice of the pump

Once the previous point has been done, one knows the value of $\frac{Q}{ur^2}$ and can compute r_D as follows:

$$\frac{Q}{ur^2} = \frac{60}{2\pi} \frac{Q}{nr^3} \quad (2.36)$$

and replacing by the design values. It is not always possible to have exact values of radius disponible for every families and one has sometimes to make compromises and thus we have to compute the final values of:

$$u_D = \frac{2\pi n_D r_D}{60} \quad \frac{Q_D}{u_D r_D^2} \quad P_m = \frac{\rho g Q_D H_D}{\eta_g} \quad (2.37)$$

where η_g is read on the curve. The rotation speed of the rotor is determined via $u_D = r\omega$.

2.5.5 Groups of pumps

Problem

For low Q and high H or high Q and low H it is possible that the desired line with ψ_D does not intersect any performance curve with an admissible efficiency. This problem can be solved using several pumps in parallel or series.

Serial grouping of pumps

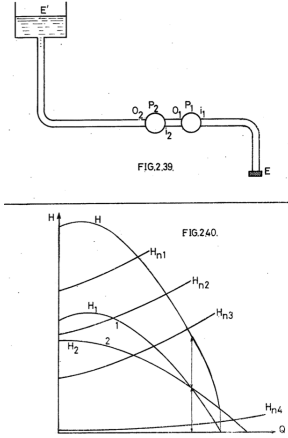


Figure 2.26

the increase in Q . For cases where high Q and low H are required, the series are limited by the maximum Q of one of the pump and thus on the figure we see that pump2 single could deliver while the combination not. In conclusion, this type is reserved for high head and low Q .

Grouping of pumps in parallel

For this case we have:

$$H = H_1 = H_2 \quad Q_1 + Q_2 = Q \quad (2.39)$$

and the graph is just obtained by the summation of the two in the Q direction. We can observe that the combination shows its interest only after a certain flow rate since for H_{n1} for example the pump1 can work alone and pumps2 is useless. In this case an anti-return valve is to be foreseen. For higher flow rates, one can observe that both pumps can deliver flow but at a lower rate. In conclusion, we see that this configuration is reserved for high flow rate applications.

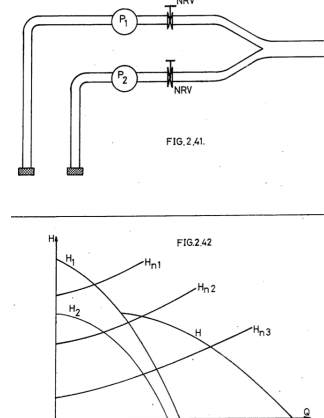


Figure 2.27

Chapter 3

Axial turbines

3.1 Stages of axial turbines

3.1.1 Organization of a stage - 2D flow

A turbine is composed of 2 main stages, the distributor with fixed vanes and the rotor (also called receptor) with rotating blades. The aim is to find the best shape for the vanes and blades in order to have the minimum flow losses. We limit ourselves to the flow through the mean cylinder (flow intersecting the blades and vanes at the mid span).

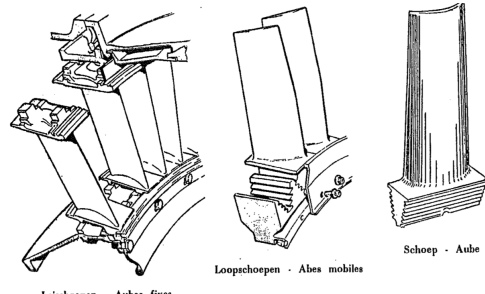
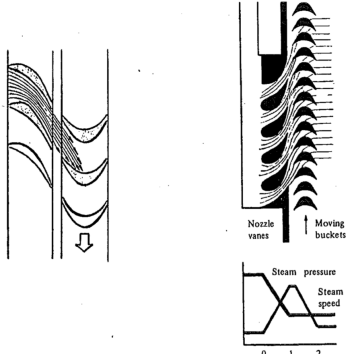


Figure 3.1

Figure 3.2

The 3D turbine will be simplified in a 2D study by considering the distributor and the receptor as a grid of blades with constant distance called **pitch** or **spacing** and a constant span h (while not in 3D) and we consider the flow identical over the span. We can end up with the first figure where we have a limited and non constant span of the blades, no presence of carter and swirling effect on the rotor not considered.

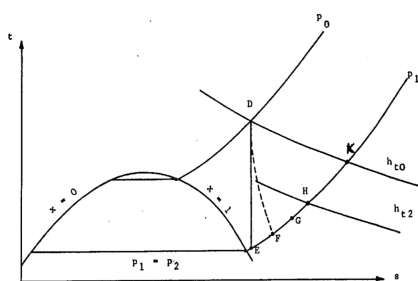


Figure 3.3

can find the total enthalpy variation through the machine.

If we look to the evolution on a T-S diagram, we know the inlet and outlet pressures, so if we define the initial state as D with p_0, t_0, v_0 , we can first consider the isentropic expansion through the stator (E). But isentropic doesn't exist so we consider the losses to arrive at F. Then we go to G through the blades since the only kinetic energy is converted into mechanical energy and not pressure. At the outlet, some kinetic energy remains and this is a loss, so we have to deduce it and arrive at point H to compute the useful energy. By drawing two iso-enthalpic curves we

3.2 Impulse stage with one velocity drop

3.2.1 Definition of the stage

The principle of this type of turbine is to first extend the ONLY flow through the vanes of the stator and then to transform kinetic energy into mechanical energy through the rotor. Since no expansion is made on rotor, the rotor blades should have the same inlet and outlet sections as shown on Figure 3.1. One can observe the velocity evolution on the same figure, where only one velocity drop happens, giving the name to the turbine.

3.2.2 Evolution of the gas/steam - Velocity triangles

Computation of the flow velocity v_1 at the outlet of the stator vanes

The expansion in the stator is the stage D to E on Figure 3.3, since the total enthalpy is conserved:

$$h_{t0} = h_{t1} \quad \Rightarrow h_0 + \frac{v_0^2}{2} = h_1 + \frac{v_1^2}{2} \quad \Rightarrow v_1 = \sqrt{v_0^2 + 2(h_0 - h_1)} \quad (3.1)$$

In fact this is not true since losses occur in reality. Let's define the reheat coefficient:

$$\zeta = \frac{h_1 - h_{1i}}{h_0 - h_{1i}} \quad (3.2)$$

where h_{1i} is the isentropic enthalpy that can be computed by laws and h_1 the real one. This is kind of efficiency factor. We have then that by making appear the equal total enthalpies (considering v_0 negligible):

$$\zeta = \frac{\frac{v_{1i}^2}{2} - \frac{v_1^2}{2}}{\frac{v_{1i}^2}{2} - \frac{v_0^2}{2}} = 1 - \left(\frac{v_1}{v_{1i}} \right)^2 = 1 - \varphi^2 \quad \Rightarrow \varphi = \sqrt{1 - \zeta} \quad (3.3)$$

where we define the **speed reduction coefficient** φ . The velocity v_1 can thus be expressed in term of h_{1i} replacing in (3.1):

$$v_1 = \sqrt{v_0^2 + 2(1 - \zeta)(h_0 - h_{1i})} \approx \varphi \sqrt{2(h_{t0} - h_{1i})} \quad (3.4)$$

where we considered v_0 negligible so that $h_0 = h_{t0}$.

Velocity triangle in section 1

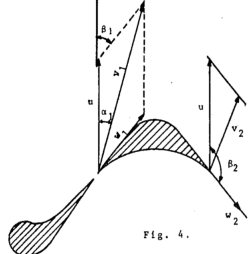


Figure 3.4

In the figure, for now we only know v_1 . But we can assume to know $u_1 = r_m \omega$ where ω is the rotation speed of the rotor and r_m the mean radius at the entrance of the wheel. To be able to compute all the triangle, we still need the angles. We will consider that in fact α_1 is an angle to fix and thus we are able to compute w_1 but also β_1 the important design angle for the rotor blades:

$$w_1^2 = v_1^2 + u_1^2 - 2u_1 v_1 \cos \alpha_1 \quad \cos \beta_1 = \frac{v_1 \cos \alpha_1 - u_1}{w_1} \quad (3.5)$$

Channel in the rotor blades - relative velocity w_2 at the receptor exit

We know that the rotor blades should be so that the pressure at inlet and outlet sections should be the same. We can also consider that $u_1 = u_2$ since it depends on the radius and the rotation speed. This applied to the kinetic energy equation we have that:

$$\frac{w_2^2 - w_1^2}{2} = -w_f'' < 0 \quad (3.6)$$

For isentropic flow, so without losses, we should have the same velocity between entrance and outlet. This is not the case in reality since we have losses and following the equation $w_2 < w_1$. Applying energy equation we see that the enthalpy increases:

$$\frac{w_2^2 - w_1^2}{2} = h_1 - h_2 \quad (3.7)$$

This was only qualitative description, to compute these outlet values, we need to know the relative velocity reduction ratio $\psi = \frac{w_2}{w_1}$ that can be known experimentally (around 0.8 - 0.9 in practice) depending on the shape of the receptor blades:

$$w_2 = \psi w_1 \quad h_2 = h_1 + \frac{w_1^2 - w_2^2}{2} = h_1 + (1 - \psi^2) \frac{w_1^2}{2} \quad (3.8)$$

Finally, in order to compute the the inlet and outlet sections, one has to use the mass flow rate equation since the velocities w are known and the density can be determined for a gas using T-S diagram point F (inlet) and G (outlet). Note that for a flow without friction, $w_2 = w_1$ and $h_2 = h_1$ so that $A_2 = A_1$ and F = G.

Shape of the rotor blades

As we have seen, in the case of no loss, $w_1 = w_2$ and the flow sections can be chosen identical. This is easily done when we give a symmetric shape to the rotor blades with the complementary solid angles $\bar{\beta}_1, \bar{\beta}_2$ (increased by 90°).

But as we have seen, in reality $w_2 < w_1$ and $\nu_2 > \nu_1$ that forces us to increase the outlet section. This is accomplished with symmetrical blades by increasing the height h of the blades between inlet and outlet.

In a pre-design phase, one will always chose $\bar{\beta}_1 = \beta_1$ the flow angle computed in the velocity triangle in order to avoid shock and separation. If the working conditions are changed further extra losses must be added.

Velocity triangle at the exit of the receptor

If we admit that we chose a symmetric blade such that $\bar{\beta}_1 = \beta_1$ and $\bar{\beta}_2 = \pi - \bar{\beta}_1$, as long as the flow in the rotor remains sane, w_2 is tangent to the blade and thus $\beta_2 = \bar{\beta}_2$. Since $u_1 = u_2$ and $w_2 = \psi w_1$, the velocity triangle is computed as:

$$v_2^2 = u_2^2 + w_2^2 - 2u_2 w_2 \cos \beta_2 \quad \cos \alpha_2 = \frac{u_2 + w_2 \cos \beta_2}{v_2} \quad (3.9)$$

Losses in the rotor channel

The lost energy corresponds to the area under the curve FG on the TS diagram, or given by the formula:

$$w''_f = h_2 - h_1 = \frac{w_1^2 - w_2^2}{2} = (1 - \psi^2) \frac{w_1^2}{2} \quad (3.10)$$

Losses at the receptor exit

At the exit, the fluid has still kinetic energy corresponding to $\frac{v_2^2}{2}$ which is lost. This energy corresponds to the projection area under GH. A part of this could be recuperated in a second stage.

3.2.3 Power on the wheel shaft (P_R)

The power on the shaft is given by the Euler-Rateau equation:

$$P_R = \dot{m}_R u (v_1 \cos \alpha_1 - v_2 \cos \alpha_2) = \dot{m}_R \left(\frac{v_1^2 - v_2^2}{2} - \frac{w_1^2 - w_2^2}{2} \right) = \dot{m}_R (\underbrace{h_{t1} - h_{t2}}_{h_{t0}}) \quad (3.11)$$

We see from this formula that the power can be computed by the total enthalpy difference. We have also:

$$P_R = \dot{m}_R \left(\frac{v_1^2 - v_2^2}{2} + \int_{p_2}^{p_1} -w_f'' \right) \Rightarrow \dot{m}_R \frac{v_1^2 - v_2^2}{2} = P_R + \dot{m}_R w_f'' \quad (3.12)$$

Where the pressure variation is null through the rotor and we see that we find the same explanations we've made. The torque applied on the blades is:

$$P_R / \omega = \dot{m}_R (v_1 \cos \alpha_1 - v_2 \cos \alpha_2) r_m \quad (3.13)$$

This shows how the variation of v in amplitude and angle gives a torque. The intersection of the iso enthalpy curve h_{t0} with $p_2 = p_1$ (point K) is represented on the same figure. The extracted energy is given by the area under HK:

$$HK = h_{t1} - h_{t2} = P_R / \dot{m}_R \quad (3.14)$$

3.2.4 Degree of reaction

By definition it is the ratio between the power of the fluid in a reactive working and the total power to the rotor:

$$R = \frac{(P_R)_{react}}{P_R} = \frac{\frac{w_2^2 - w_1^2}{2}}{\frac{v_1^2 - v_2^2}{2} + \frac{w_2^2 - w_1^2}{2}} = \frac{\int_{p_2}^{p_1} \nu dp - w_f''}{\frac{v_1^2 - v_2^2}{2} + \int_{p_2}^{p_1} \nu dp - w_f''} \approx 0 \quad (3.15)$$

This is nearly 0 since the difference in v is very small and the pressure constant over the blade. It would be strictly 0 if there was no friction, this is why this kind of blade is an impulse or action stage.

3.2.5 Stage efficiency – Pre-design

Stage efficiency

This is by definition the ratio of the power of the stage (delivered to the rotor) and the theoretical available power that is obtained by product of \dot{m}_R with the kinetic energy available after isentropic and complete expansion, and no remaining energy at the exit of the rotor. The theoretical power and the efficiency are:

$$\dot{m}_R \frac{v_{1i}^2}{2} = \dot{m}_R(h_{t0} - h_{1i}) \quad \Rightarrow \eta_E = \frac{\dot{m}_R u(v_1 \cos \alpha_1 - v_2 \cos \alpha_2)}{\dot{m}_R \frac{v_{1i}^2}{2}} = \frac{h_{t0} - h_{t2}}{h_{t0} - h_{1i}} = \eta_D \eta_R \quad (3.16)$$

also the product of distributor and rotor efficiency since $\frac{\dot{m}_R \frac{v_{1i}^2}{2}}{\dot{m}_R \frac{v_{1i}^2}{2}} \cdot \frac{\dot{m}_R u(v_1 \cos \alpha_1 - v_2 \cos \alpha_2)}{\dot{m}_R \frac{v_{1i}^2}{2}}$. Previously

we said α_1 and u are chosen, let's see how to choose the most efficient. If $\bar{\beta}_1$ is chosen tangent to w_1 , there is no shock and thus the coefficient of reduction $\psi = \psi_r$ depends on the friction in the rotor. Then, if one consider a symmetric blade, these relations in the velocity triangle can be made:

$$v_2 \cos \alpha_2 = u + w_2 \cos \beta_2 = u - \psi_r w_1 \cos \beta_1 = u - \psi_r (v_1 \cos \alpha_1 - u) \quad (3.17)$$

and after replacing in the definition of $\eta_E = \eta_D \eta_R$:

$$\eta_E = 2\eta_D \frac{u}{v_1} \left[\cos \alpha_1 - \frac{u}{v_1} + \psi_r \left(\cos \alpha_1 - \frac{u}{v_1} \right) \right] = f(\eta_D, \alpha_1, \frac{u}{v_1}, \psi_r) \quad (3.18)$$

where $\eta_D = \frac{v_{1i}^2}{v_{1i}^2} = \varphi^2 = 1 - \zeta$ as demonstrated previously. We define $\xi = \frac{u}{v_1}$ as the **speed coefficient** and thus:

$$\eta_E = 2\eta_D \xi (1 + \psi_r) (\cos \alpha_1 - \xi) \quad (3.19)$$

Optimal values of the elements in the velocity triangles

η_D depends on α_1 related to the camber of the distributor blades, on v_1 depending on the pressure drop P_0/P_1 that depends on the shape of the distributor (convergent/divergent). The velocity coefficient ψ is also function of α_1 and v_1 since it depends on the difference $\bar{\beta}_2 - \bar{\beta}_1$. ψ_r depends also on w_1 . Due to lack of information, we can just suppose that since these parameters are limited η_D and ψ are constant and we will try to optimize using ξ and α_1 .

The maximum stage efficiency η_E in function of ξ is obtained for null derivative (do it as exercise it's ok for me):

$$\xi_{opt} = \frac{\cos \alpha_1}{2} \quad \Rightarrow \eta_E = 2\eta_D (1 + \psi_r) \xi_{opt}^2 \quad (3.20)$$

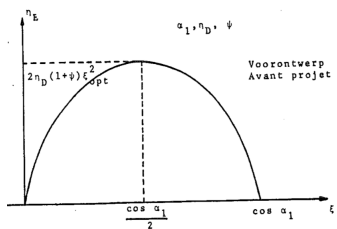


Figure 3.5

On basis of this, we can see that the maximum efficiency is obtained for maximum $\cos \alpha_1$ and thus minimum α_1 . But small α_1 means smaller axial component, larger vertical component, larger flow section required and thus longer vanes/blades. Moreover, the stator vanes must have higher curvature and larger chord. This is negative effects and the angle is chosen between 15-25° in practice. The evolution of η_E in function of ξ

is shown on the figure. The value of η_D is around 0.9-0.96, ψ_r between 0.8-0.95 for $\alpha_1 \approx 20^\circ$ and the maximum stage efficiency is around 0.8.

Selection of a speed coefficient different from the optimum

We have seen that there is an optimal value for $\xi = \frac{u}{v_1}$ of $\frac{\cos \alpha_1}{2}$. If the pressure drop in the stage is such that the optimum value of u is unacceptable:

$$u_{opt} = \frac{v_1 \cos \alpha_1}{2} \approx \frac{v_1}{2} \quad (3.21)$$

due to material stresses or temperature constraints. The maximal value of u is dictated by the material and the design and is normally between 250-300 m/s but can go up to 400 m/s with special alloys. In some cases we can thus be forced to use lower efficiency than the maximum one. Till now, we have considered that the flow was always tangent to the blades and thus we forgot some losses, let's see what happens in off-design condition.

3.2.6 Performance in off-design condition

Influence on the stage efficiency

A turbine is not always working in the conditions it has been design for. For example, it can be designed for a pressure ratio $(p_0/p_1)_d$ (selection of convergence or divergence) but whatever the reason if the ratio changes during the operations:

- If we have a convergent-divergent, the distributor efficiency will drop because the geometry is rather different that it should be in off design conditions.
- If the distributor channels are simply convergent, the flow will adapt itself to the existing geometry and the efficiency will not be so much perturbed, as long as $p_0/p_1 < p_0/p_c$ (critical pressure).

If the working conditions change in u or v , the efficiency is not so much affected as long as the ratio $\frac{u}{v_1}$ stays identical to $\frac{u_d}{v_{1d}}$. If it is not the case, the flow angle β_1 will be different from the solid angle $\bar{\beta}_1$ and shocks will appear, inducing more losses and thus lower velocity at the output of the rotor blade. This is taken into account via a new coefficient ψ_i :

$$w_2 = \psi_r \psi_i w_1 \quad (3.22)$$

As long as the off design conditions does not differ too much from the initial ones, w_2 can be assumed to remain tangent. When the real value of $\eta_D < \eta_{Dd}$ and $\psi < \psi_d$ are determined by off design testing, the stage efficiency can be computed after establishing the new velocity triangle:

$$\eta_E = 2\eta_D \frac{u(v_1 \cos \alpha_1 - v_2 \cos \alpha_2)}{v_1^2} \quad (3.23)$$

It is in fact rather difficult because there is a lack of quantitative information about η_D and ψ .

Stage characteristics

The stage characteristic is a curve of the torque T_R on the wheel/shaft in function of the rotation speed N or tangential velocity $u = r\omega$ at a given \dot{m}_R , a given Δp through the stage and a given temperature:

$$T_R = \frac{P_R}{\omega} = \dot{m}_R(v_1 \cos \alpha_1 - v_2 \cos \alpha_2)r_m \quad (3.24)$$

If we can accept that $\beta_2 = \bar{\beta}_2$:

$$v_2 \cos \alpha_2 = u - \psi w_1 \cos \beta_1 \Rightarrow T_R = \dot{m}_R(v_1 \cos \alpha_1 - u + \psi w_1 \cos \beta_1)r_m \quad (3.25)$$

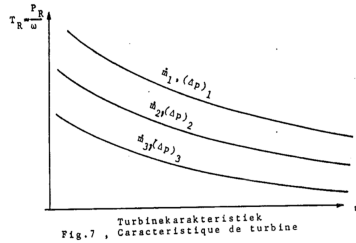


Figure 3.6

3.2.7 Pressure drop in the optimum conditions

We have seen that the maximum stage efficiency is obtained for

$$\xi = \frac{u}{v_1} = \frac{\cos \alpha_1}{2} \approx \frac{1}{2} \quad (3.26)$$

Using the relation we found for v_1 previously we can compute the best value of u as:

$$v_1 = \sqrt{2(1 - \zeta)(h_0 - h_{1i})} \Rightarrow u = 0.5\sqrt{2(1 - \zeta)(h_0 - h_{1i})} \quad (3.27)$$

u has a maximum value and implies thus that one could have to limit the enthalpy variation $h_0 - h_{1i}$ in order to stay in maximum efficiency range.

3.3 Impulse stage with two velocity drops or two-stage impulse turbine

3.3.1 Need for two velocity drop

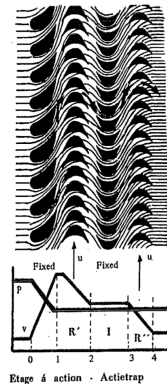
When the pressure drop and thus enthalpy drop is too large, v_1 is too large since:

$$v_1 = \sqrt{2(1 - \zeta)(h_0 - h_{1i})} \quad (3.28)$$

This is not good for the best efficiency since u should be such that $\xi \approx 0.5$. This can be explained by the fact that the kinetic energy at the end of the receptor is too high and is lost. The goal of the second stage is to recuperate this lost energy.

3.3.2 Organization and way of working

It is constituted of two stages now. We have a fixed distributor expanding the gas from p_0 to p_1 and the velocity increases from $v_0 \approx 0$ to v_1 . The pressure remains constant in the rest of the stages. A first rotor R' transforms part of the kinetic energy $\frac{v_1^2}{2}$ into mechanical work. It is followed by an inverter I that orientates the flow in the right direction to go into the second rotor R'' . It is mandatory if the rotors are connected on the same shaft, if they are allowed to turn in opposite direction it is not. The output kinetic energy is lower than a one stage $\frac{v_2^2}{2} < \frac{v_1^2}{2}$ and thus the losses are less. The disadvantage is that the inverter is a loss.



3.3.3 Evolution of the fluid – velocity triangles

Absolute velocity at the exit of the distributor

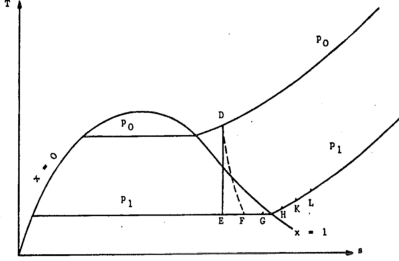


Figure 3.8

then be computed.

If we resketch the TS diagram as previous case, the initial conditions are characterized by a pressure p_0 , velocity v_0 often negligible and temperature T_0 . If one knows p_1 and the reheat coefficient ξ or reduction ψ it is easy to find v_1 .

Velocity triangle in section 1

This is the same as previously, if we can fix α_1 and the tangential velocity u_1 one can build the velocity triangle at the input of the rotor. The angle β_1 and the velocity w_1 can

Shape of the rotor blades – Relative velocity at the exhaust

The pressure is conserved and the relative velocity decreases in the rotor as:

$$w_2 = \psi' v_1 \quad (3.29)$$

where ψ' is the velocity reduction in the first rotor. One then computes the enthalpy drop since the total enthalpy is constant:

$$h_2 = h_1 + \frac{w_1^2 - w_2^2}{2} \quad (3.30)$$

One can thus define the point G in the T S diagram after the evolution FG. The blades are assumed to be symmetric and in design condition $\beta_1 = \beta_1$.

Velocity triangle in section 2

Since the blades are symmetric $\bar{\beta}_2 = 180^\circ - \bar{\beta}_1$ and $u_2 = u_1$, w_2 is known using ψ' allows to compute v_2 and α_2 .

Blade shape of the second rotor

The inlet angle β_3 is chosen equal to the exit angle β_3 of the inverter blades. It is larger than β_1 , less curvature and thus less friction loss. The blades are again symmetric.

Velocity triangle in exhaust section 4

As the previous blade, the velocity reduction coefficient is known:

$$w_4 = \psi'' w_3 \quad (3.31)$$

The enthalpy drop can be computed:

$$h_4 = h_3 + \frac{w_3^2 - w_4^2}{2} = h_3 + w_3^2 \frac{1 - \psi''^2}{2} \quad (3.32)$$

As previously we can build the velocity triangle thanks to the symmetry and find the evolution HK on the diagram.

Loss at the exit of the stage

There is still a certain velocity remaining at the exit of the total turbine, this is represented by point L:

$$h_{t4} = h_4 + \frac{v_4^2}{2} \quad (3.33)$$

3.3.4 Power P_R on the rotor

The power is just the sum of what we have with Euler-Rateau individually:

$$P'_R = \dot{m}'_R u(v_1 \cos \alpha_1 - v_2 \cos \alpha_2) = \dot{m}'_R (h_{t1} - h_{t2}) \quad P''_R = \dot{m}''_R u(v_3 \cos \alpha_3 - v_4 \cos \alpha_4) = \dot{m}''_R (h_{t3} - h_{t4}) \quad (3.34)$$

where if we suppose that $\dot{m}'_R = \dot{m}''_R = \dot{m}_R$ and by the isentropic expansion that $h_{t1} = h_{t0}$ and $h_{t3} = h_{t2}$:

$$P_R = P'_R + P''_R = \dot{m}_R (h_{t0} - h_{t4}) \quad (3.35)$$

3.3.5 Stage efficiency – Pre-design of the stage

Definition of the 2 stages efficiency

As we have done previously, let's define the efficiency as the ratio between the power on the rotor and the power that enters theoretically:

$$\eta_E = \frac{\dot{m}_R (h_{t0} - h_{t4})}{\dot{m}_R (h_{t0} - h_{1i})} = \frac{\dot{m}_R (v_1 \cos \alpha_1 - v_2 \cos \alpha_2 + v_3 \cos \alpha_3 - v_4 \cos \alpha_4)}{\dot{m}_R \frac{v_{1i}^2}{2}} \quad (3.36)$$

where again we could multiply and divide by v_{1i}^2 to make appear the distributor efficiency $\frac{v_1^2}{v_{1i}^2}$. For what concerns the angles, they can be found by computing the velocity triangles using u, ψ, v_1, α_1 . Be cautious that we assumed the stage to be without shock so the value of ψ only depends on the blades shape (symmetric). To find the best u, v_1 and α one has to express the stage efficiency like:

$$\eta_E = f(\eta_D, u/v_1, \alpha_1, \psi', \psi_I, \psi'') \quad (3.37)$$

Computation of the 2-stage efficiency

Since all sections velocity triangle depends on the previous one, we could apply the previous section discussion as:

$$v_4 \cos \alpha_4 = u + w_4 \cos \beta_4 = u - \psi'' w_3 \cos \beta_3 = u - \psi'' (v_3 \cos \alpha_3 - u) \quad (3.38)$$

and following the same way:

$$v_3 \cos \alpha_3 = -\psi_I v_2 \cos \alpha_2 \quad v_2 \cos \alpha_2 = u - \psi' (v_1 \cos \alpha_1 - u) \quad (3.39)$$

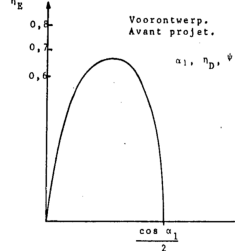
Replacing all the terms and making appear the speed coefficient $\xi = u/v_1$, we find:

$$\eta_E = 2\eta_D \xi \left[(1 + \psi') (\cos \alpha_1 - \xi) - (1 + \psi_I) (1 + \psi'') \xi + (1 + \psi'') \psi_I \psi' (\cos \alpha_1 - \xi) \right] \quad (3.40)$$

In reality the reduction coefficients are not the same, $\psi'' > \psi'$, but for simplicity consider them equal:

$$\eta_E = 2\eta_D(1 + \psi)\xi[(1 + \psi^2) \cos \alpha_1 - (2 + \psi + \psi^2)\xi] \quad (3.41)$$

Triangle of the optimal velocities in section 1



As previously, we will assume that ψ and η_D are constant for small variation of α_1 so that the stage efficiency is only function of $\eta_E = \eta_E(\alpha_1, \xi)$. With derivation:

$$\xi_{opt} = \frac{(1 + \psi^2) \cos \alpha_1}{2(2 + \psi + \psi^2)} \approx \frac{\cos \alpha_1}{4} \Rightarrow \eta_{E_{max}} = \eta_D(1 + \psi)(1 + \psi^2)\xi_{opt} \quad (3.42)$$

Figure 3.9
The efficiency is 0 for $\xi = 0$ and for $\xi = 2\xi_{opt}$.

3.3.6 Performance of an existing stage in off-design conditions

The discussion is the same, since we are not in design condition the $\beta_1, \alpha_2, \beta_3$ are different from the $\bar{\beta}_1, \bar{\alpha}_2, \bar{\beta}_3$ and it is necessary to introduce ψ_i in the $\psi = \psi_i \psi_r$ to take into account the shocks at the entrance sections. As far as the flow remains "clean" (follows the direction of the blades) for the exits, one admits that:

$$\alpha_1 = \bar{\alpha}_1 \quad \alpha_2 = \bar{\alpha}_2 \quad \alpha_3 = \bar{\alpha}_3 \quad (3.43)$$

One is then able to compute the velocity triangle and to use the formula for the efficiency to get it. The stage characteristics $T_R(N)$ are as previously decreasing functions of N .

3.3.7 Optimum speed coefficient and pressure drop

The ξ_{opt} is a bit lower than 0.25. By neglecting v_0 in the expression of v_1 :

$$v_1 = \sqrt{2(1 - \zeta)(h_0 - h_{1i})} \quad \Rightarrow u = 0.25\sqrt{2}\varphi\sqrt{(h_0 - h_{1i})} \quad (3.44)$$

where φ is the velocity reduction coefficient of the distributor. Since u is limited (lower than 300 m/s), the isentropic enthalpy drop and thus the pressure drop must be limited.

3.4 Impulse stage with three velocity drops

If the enthalpy variation and the pressure drop are extremely high, the kinetic energy at the exit of the second rotor could be still high and this is lost. We could add one stage to recuperate it. Following the same reasoning as previous case, we find the following optimum coefficient:

$$\xi_{opt} \approx \frac{\cos \alpha_1}{8} \approx 0.125 \quad (3.45)$$

For this value, η_E reaches 50%.

3.4.1 Comparison between the three types of impulse stages

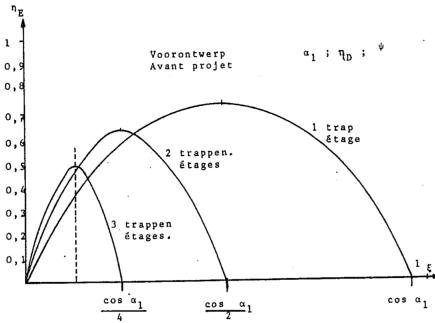


Figure 3.10

We have seen that the optimal value of the velocity coefficient is decreasing with the number of stages this is interesting for high isentropic enthalpy drops. Nevertheless, the efficiency is also decreasing. This imposes that the number of stage is never exceeding 3. On the figure, we can see that between 0 and $\cos \alpha_1/8$, the difference in efficiency between the two and three stages is minimal but the cost of the three is much higher. It can be thus more interesting to work with a 2 stages.

3.5 Turbine reaction stage

3.5.1 Organization

Previously we saw the impulse stage for which the only pressure drop happens in the stator. The reaction turbine is composed of a ring of stationary blades called the stator vanes such, place of the first expansion (set of nozzle) from p_0 to p_1 inducing a kinetic energy increase $\frac{v_1^2}{2} > \frac{v_0^2}{2}$. The second step is a ring of rotating blades called rotor, where both the pressure and kinetic energy are converted into mechanical energy. This is strictly different from the previous case since the pressure also contributes now.

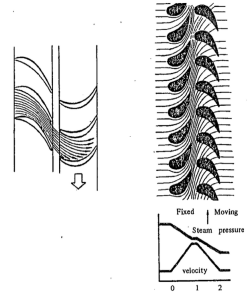


Figure 3.11

3.5.2 Transformations and velocity triangles

Stator vanes (distributor)

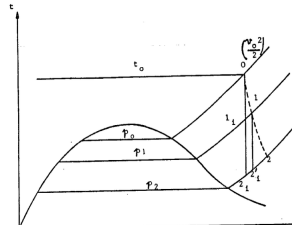


Figure 3.12

As always, the figure represents the TS diagram, we are at state 0. The velocity at the end of transformation 0-1 is given by total enthalpy conservation:

$$v_1 = \sqrt{v_0^2 + 2(h_0 - h_1)} = \sqrt{v_0^2 + 2(1 - \zeta)(h_0 - h_{1i})} \quad (3.46)$$

- The v_0 we neglected previously can no longer be neglected for reaction turbines, at least usually.

Inlet section of rotor – rotor blades

Same as before, we know α_1, u_1 , so we can build the triangle and determine w_1, β_1 . The kinetic energy and the energy conservation equations in rotating frame were:

$$\frac{w_2^2 - w_1^2}{2} = - \int_{p_1}^{p_2} \nu dp - w_f'' \quad \frac{w_2^2 - w_1^2}{2} = h_1 - h_2 \quad (3.47)$$

As $u_2 = u_1$ on a same blade, the equations are the same as non rotating frame but with w instead of v . We see that since $dp < 0$, $w_2 > w_1$. If the losses $w_f'' = 0$, the expansion on the rotating blades are represented by 1-2'_i on previous figure. It is never the case in reality so we have to find 1-2. This is done by considering the reheat coefficient:

$$\zeta'' = \frac{h_2 - h'_{2i}}{h_1 - h'_{2i}} \Rightarrow h_2 - h_1 = (1 - \zeta'')(h_1 - h'_{2i}) = \frac{w_2^2 - w_1^2}{2} \quad (3.48)$$

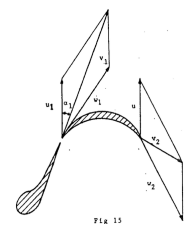


Figure 3.13

For what concerns the shape of the blades, during a pre-design step, we generally choose $\bar{\beta}_1 = \beta_1$. The relative velocity at the inlet of the rotor is subsonic, we must design a convergent or convergent-divergent nozzle type inter-blade channel design.

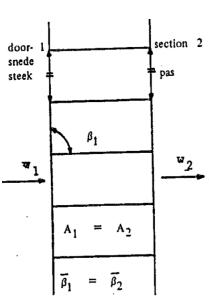


Figure 3.14

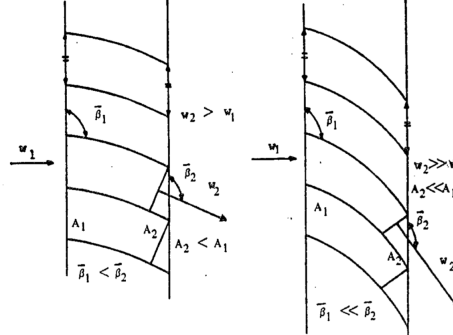


Figure 3.15

Since the inlet flow is subsonic, convergent nozzles are used to obtain an outlet flow with $w_2 < w_1$. The two figures above clearly shows that the cross-sectional area depends on the angles $\bar{\beta}_1, \bar{\beta}_2$. Since the distance between the blades is the same at inlet and outlet sections, one must play on the blade height. When $\bar{\beta}_1 = \bar{\beta}_2$ we have that $A_1 = A_2$ and thus $w_2 = w_1$. If $\bar{\beta}_1 < \bar{\beta}_2$, the cross-sectional area in the direction of the flow is decrease, while the vertical distance between the blades remains constant. When $\bar{\beta}_2$ decreases, w_2 increases, but the distance achieved by the flow in the inter-blade channel is also increase, this increases the friction losses.

Velocity triangle at the outlet of the rotor blades

Since one knows u_2, w_2 and β_2 (chosen = $\bar{\beta}_2$), it is possible to compute v_2 and α_2 .

3.5.3 Losses - Recovery

Energy losses in the inter-blade channel of the stator is given by:

$$\frac{v_{1i}^2 - v_i^2}{2} = h_1 - h_{1i} \quad (3.49)$$

and is represented by the projection area 1_{i1} . The inter-blade channel loss in the rotor is represented by projection area $2'_{i2}$. If we compare the sum of these losses and the loss of the stage 2_{i2} , one can remark that the projection area 2_{i2} is lower. This means that part of the stator losses are recovered in the stage. This can be explained by the fact that friction in the stator converts the energy into heat, that is then recovered in the rotor.

3.5.4 Power delivered to the rotor

The delivered power is given by the Euler-Rateau equation:

$$P_R = \dot{m}_R u (v_1 \cos \alpha_1 - v_2 \cos \alpha_2) = \dot{m}_R \left[\frac{v_1^2 - v_2^2}{2} + \int_{p_1}^{p_2} \nu dp \right] - w_f'' \quad (3.50)$$

where we clearly see the contributions of kinetic energy and of pressure drop. Knowing that $v_1 \cos \alpha_1 = u + w_1 \cos \beta_1$ and $v_2 \cos \alpha_2 = u + w_2 \cos \beta_2$, one can see the importance of the angles β on the torque P_R/ω . If we have the first config on Figure 3.14, there will be no torque while those on Figure 3.15 will induce torque.

3.5.5 Degree of reaction

It has been previously defined as:

$$R = \frac{(P_R)_{react}}{P_R} = \frac{\frac{w_2^2 - w_1^2}{2}}{\frac{v_1^2 - v_2^2}{2} + \frac{w_2^2 - w_1^2}{2}} = \frac{\int_{p_2}^{p_1} \nu dp - w_f''}{\frac{v_1^2 - v_2^2}{2} + \int_{p_2}^{p_1} \nu dp - w_f''} \approx 0 \quad (3.51)$$

This ratio is clearly different from 0 since there is now pressure variation in the rotor. If it is higher than 1 we speak about **superreaction stage**.

3.5.6 Parsons turbine reaction stage

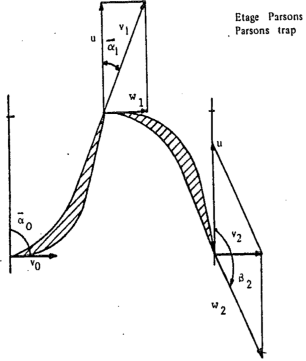


Figure 3.16

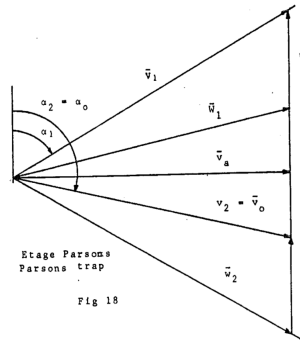


Figure 3.17

Frequently, the design of the rotor and the stator blades are the same, however the rotor blades rotates from 180° around their symmetry line:

$$\bar{\beta}_1 = \pi - \bar{\alpha}_0 \quad \bar{\beta}_2 = \pi - \bar{\alpha}_1 \quad (3.52)$$

The blade height is selected such that the axial velocity is constant over the stage $v_2 = v_0$. Velocity triangle at the inlet and outlet of the rotor blades are symmetric with regard to the axial direction. Therefore:

$$v_0 = v_2 = w_1 \quad v_1 = w_2 \quad \bar{\alpha}_0 = \bar{\alpha}_2 \quad (3.53)$$

When a Parsons turbine is composed of multiple stages, all the rotors and stators have the same shape, only the blade heights are different. Consider this type of turbine for the next sections.

3.5.7 Degree of reaction of Parsons turbine - Enthalpy drop

Using the velocity triangle in the definition of degree of reaction is = 0.5. The enthalpy drop in the stator and the rotor is given by:

$$h_0 - h_1 = \frac{v_1^2 - v_0^2}{2} = \frac{v_1^2 - v_2^2}{2} \quad h_1 - h_2 = \frac{w_2^2 - w_1^2}{2} \quad \Rightarrow h_0 - h_1 = h_1 - h_2 \quad (3.54)$$

The real enthalpy drop in rotor and stator are the same. As the rotor and stator blades are the same, the reheat coefficients are almost the same $\zeta' \approx \zeta''$. But:

$$h_0 - h_{1i} = \frac{h_0 - h_1}{1 - \zeta'} \quad h_1 - h_{2'i} = \frac{h_1 - h_2}{1 - \zeta''} \quad \Rightarrow h_0 - h_{1i} = h_1 - h_{2'i} \quad (3.55)$$

The isentropic enthalpy drops are equal. Moreover, since on previous TS diagram 1 and 1*i* where very close, we can assume $h_0 - h_{1i} = h_{1i} - h_{2i}$. In conclusion, the pressure drop in the stage is almost equally distributed between the stator and rotor.

3.5.8 Stage efficiency and pre-design study

Stage efficiency

The stage efficiency definition is:

$$\eta_E = \frac{\dot{m}_R(h_{t_0} - h_{t_2})}{\dot{m}_R(h_{t_0} - h_{2i})} = \frac{u(v_1 \cos \alpha_1 - v_2 \cos \alpha_2)}{\frac{v_0^2}{2} + h_0 - h_{2i}} \quad (3.56)$$

The velocity triangles and the enthalpy drops in the stator and the rotor can be determined by knowing v_1, u, α_1 . Therefore we will express η_E in function of these. Consider angles = to solid angles, we know that:

$$\begin{cases} h_0 - h_{2i} = 2(h_0 - h_{1i}) = 2\frac{h_2 - h_1}{1 - \zeta'} = \frac{v_1^2 - v_2^2}{1 - \zeta'} \\ v_2 \cos \alpha_2 = u + w_2 \cos \beta_2 = u - v_1 \cos \alpha_1 \\ v_0^2 = w_1^2 = u^2 + v_1^2 + 2uv_1 \cos \alpha_1 \end{cases} \Rightarrow \eta_E = \frac{2\xi(2 \cos \alpha_1 - \xi)}{1 + \frac{1+\zeta'}{1-\zeta'}\xi(2 \cos \alpha_1 - \xi)} = \frac{2}{\frac{1+\zeta'}{1-\zeta'} + \frac{1}{\xi(2 \cos \alpha_1 - \xi)}} \quad (3.57)$$

The very last expression is not derived in the syllabus but is given as another form to simplify the following discussion.

Optimization of α_1 and ξ

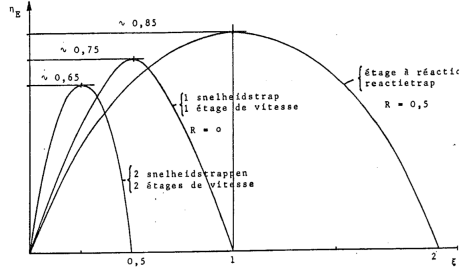


Figure 3.18

ζ depends on the curvature of the flow, if we neglect these effects, one can assume that ζ is constant. Looking to η_E formula shows that it will be maximum for α_1 as low as possible and for $\xi = \cos \alpha_1 \approx 1$. $\eta_E = 0$ for $\xi = 0$ and $\xi = 2 \cos \alpha_1$. The expression of the maximum efficiency is:

$$\eta_{E_{max}} = \frac{2(1 - \zeta) \cos^2 \alpha_1}{1 - \zeta + (1 + \zeta) \cos^2 \alpha_1} \quad (3.58)$$

3.5.9 Off-design operation of the stage

He passed this section but I did it

When the stage pressure drop $p_0 - p_2$ is different from the design one, or if $u \neq u_d$ then the velocity triangles will change and angles too, therefore shocks appear. This is as always taken into account with the slowdown coefficients ψ'_i, ψ''_i that decreases when the difference $|\alpha_0 - \bar{\alpha}_0|, |\beta_1 - \bar{\beta}_1|$ increases. The kinetic energy losses at the inlet are given by:

$$(1 - \psi'_i)^2 \frac{v_0^2}{2} \quad (1 - \psi''_i)^2 \frac{w_1^2}{2} \quad (3.59)$$

Flow velocities at the outlet, taking into account the shocks are given by:

$$v_1 = \sqrt{(\psi'_i v_0)^2 + (1 - \zeta')(h_0 - h_{1i})} \quad w_2 = \sqrt{(\psi''_i w_1)^2 + (1 - \zeta')(h_1 - h_{2'i})} \quad (3.60)$$

If the operating conditions are not too far from the design ones, the flow angles at the outlet can be assumed to be identical to the solid ones $\alpha_1 = \bar{\alpha}_1, \beta_2 = \bar{\beta}_2$. Once one has fixed the different coefficients, it is possible to determine the velocity triangles and to compute:

$$\eta_E = \frac{u(v_1 \cos \alpha_1 - v_2 \cos \alpha_2)}{h_0 - h_{2i}} \quad \frac{P_R}{\omega} = \dot{m}_R (v_1 \cos \alpha_1 - v_2 \cos \alpha_2) r_m \quad (3.61)$$

The stage characteristics is a decreasing curve as always.

3.6 Comparative study of the stage types

3.6.1 Optimum velocity coefficient

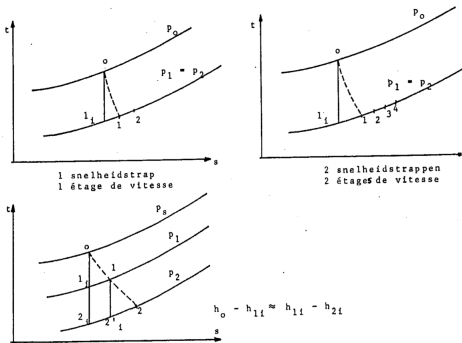


Figure 3.19

The 1 velocity drop, 2 velocity drop and Parsons stages TS diagram are depicted on the figure. The isentropic enthalpy drops $0-1_i$ and $0-2_i$ are called Δh_{is} . The optimum velocity coefficient for the three stages are respectively $\approx 1/2, \approx 1/4, \approx 1$. If one assumes that the reheat coefficient is the same for all the stages and equal to ζ and if v_0 is neglected (rougher approximation for Parsons), then the general formula:

$$v_1 = k \sqrt{h_0 - h_{1i}} \quad \Rightarrow u = \xi_{opt} k \sqrt{h_0 - h_{1i}} \quad (3.62)$$

where $h_0 - h_{1i} = \Delta h_{is}$ for 1 and 2 velocity drops and $\Delta h_{is}/2$ for Parsons, such that for the three different stages we have:

$$u_1 \approx \frac{1}{2} k \sqrt{\Delta h_{is}} \quad u_2 \approx \frac{1}{4} k \sqrt{\Delta h_{is}} \quad u_{par} \approx \frac{1}{\sqrt{2}} k \sqrt{\Delta h_{is}} \quad \Rightarrow u_2 < u_1 < u_{par} \quad (3.63)$$

What is even more important is to compare the enthalpy drops that can be used by fixing u_{max} to all stages. By isolating Δh_{is} in the previous formulas:

$$\Delta h_{is,1} = \frac{4u^2}{k^2} \quad \Delta h_{is,2} = \frac{16u^2}{k^2} \quad \Delta h_{is,1} = \frac{2u^2}{k^2} \quad (3.64)$$

We can see that the 2 velocity drops stage enthalpy drop is 4 times higher than the impulse stage with one velocity drop and 8 times higher than the reaction turbine. They are thus suited to obtain large enthalpy drops with a small number of stages, they are more **compact**. The Parsons turbine is used for high efficiency in non-continuously operated applications.

3.6.2 Stage efficiency

The previous efficiency figure shows clearly that the highest efficiency in optimal velocity coefficient is obtained with the Parsons turbine. When going in off-design conditions, the curves on Figure 3.18 are a good illustration of the shape of the curves but we are beyond the curves on left and right (more losses). We can see that for small variations around the maximum point, the Parsons turbine shows a much better **flexibility**, the curve is flatter than the impulse stages.

Chapter 4

Hydraulic turbines

4.1 Introduction

4.1.1 Definition

The major difference with gas turbines is the reversibility of the system when the degree of reaction is higher than 0 (0.5 for example). It can work as a pump and as a turbine. This has an application in hydraulics and not in gas, this is why it is more important in this case.

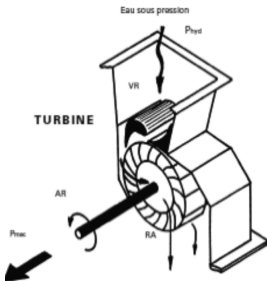
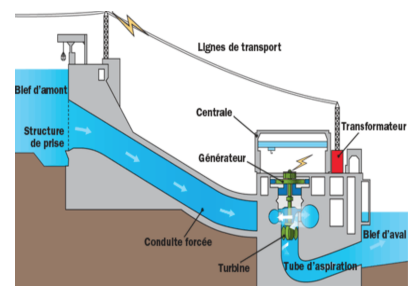


Figure 4.1

and small declivities.

Rotor preceded by a convergent entrance, connected on a shaft and we put an alternator to produce electricity. Here we see that it is very strange because we have seen axial and centrifugal machines, here we have a mixture of these. We transform the potential energy in kinetic energy before the rotor, then we transform it (+ pressure energy) into mechanical energy, with a continuous flow. If we look at the applications, 110 MW is produced by hydraulic turbines in Belgium, this is rather small compared to wind turbines production for example. It could be much higher, but for that we need to have large river and large declivities. In Belgium we have only small river

The other problem is that the rivers are dirty and it is strictly forbidden to kill any fish, for that the turbine has to be put in a channel along the river. We have also PHES systems that are in fact large water reservoirs that are filled and used to provide electricity in emergency or start nuclear power plants. These systems are very good for environment but not very profitable.



4.1.2 Basic notions

The hydraulic power is given by:

$$P_{hyd} = \rho Q g H \quad (4.1)$$

where Q is the discharge volumetric flow rate and H the net water head. We see that for a height of 10 m and a flow of $1 \text{ m}^3/\text{s}$ we only have 100 kW of power. This is very low.

4.1.3 Mechanical power turbine shaft

For what concerns the mechanical power, the pressurized water entering the rotor produces hydrodynamic force on the blades which gives a torque:

$$P_{mec} = T\omega \quad (4.2)$$

4.1.4 Efficiency of a turbine

What is important is to have a rather flat high efficiency region since the volumetric flow rate is not always constant in rivers etc (60-90% of Q_{max} in general):

$$\eta_t = \frac{P_{mec}}{P_{hyd}} \quad (4.3)$$

4.1.5 Specific speed of a turbine

There are two different specific speeds used to classify turbines based on their performances. They are obtained by non-dimensionalizing with similarity laws. We have the **specific speed** N_s which is related to the power, it is the rpm of a turbine working under a fall of 1m and delivering a power of 1kW:

$$N_s = n \frac{P^{1/2}}{H^{5/4}} \quad (4.4)$$

There is also **Nq** which is characteristic of the flow rate. It is the rpm of a turbine working under a fall of 1m and a flow rate of $1 \text{ m}^3/\text{s}$:

$$N_q = n \frac{Q^{1/2}}{H^{3/4}} \quad N_s \approx 3N_q \quad (4.5)$$

4.2 Impulse turbines

They cannot be used in reversed mode since they have a null degree of reaction. We must find again 0 pressure drop in the rotor and symmetrical blades. The principle is simple, we have a free jet going through a convergent nozzle and acting on blades placed at the periphery of a wheel. The characteristics are the preconversion of potential energy into kinetic energy before the rotor, conversion of kinetic energy into mechanical energy keeping constant pressure, and the wheel is not completely submerged.

4.2.1 Pelton turbines

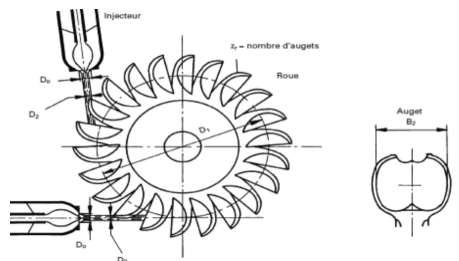


Figure 4.3

The water strikes the buckets half-symmetrically to the edge that separates them. There is a deflector that moves quickly between the injector and the rotor to deflect the jet to avoid overspeed in case of sudden setting off of the generator. The injector consists in a convergent nozzle forming a compact water jet at high speed and a movable needle for flow control. There exists also the **Turgo turbine** which is a Pelton with spoon shaped buckets and an injection inclination of 20°.

There exists two configuration related to the shaft direction: horizontal or vertical axis. The problem with the horizontal axis is that the generator can be in contact with water while in vertical axis configuration it can be put on top to avoid humidity. Jet number is limited to 2 and 6 respectively.

It is suitable for medium to high heads (30m to 1000m) and low flow rates (0.2 to $2 \text{ m}^3/\text{s}$), N varies between 500 and 1500 rpm ($N_g = 2 \dots 30$). The pros and cons are as:

- + The efficiency is about 85% and satisfactory on a wide range of Q (20% to 100% of Q_{max} for 1 injector, from 10% with 2).
- + High speed so directly coupled to the generator.
- + Simple to build, compact, robust.
- Requirement of high accuracy in the manufacture of certain parts.
- Low inertia may require a flywheel.

4.2.2 Cross-flow or Banki-Mitchell turbines

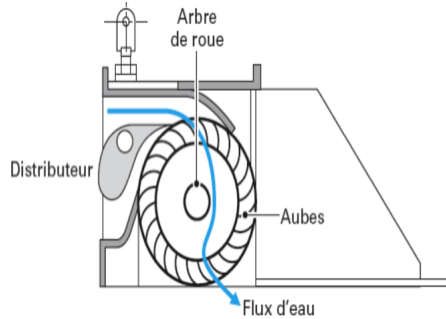


Figure 4.4

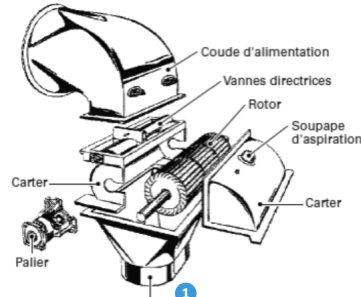


Figure 4.5

The flow acts centripetally at the entrance and centrifugally at the output of the rotor (2 strikes). The distributor is a nozzle with rectangular cross-section and is similar to a butterfly valve to control the inflow. This may be the solution to low head (3 - 200 m) and high flow rate (0.3 - $9 \text{ m}^3/\text{s}$) configurations ($N_g = 2 \dots 30$). But when the head is too low or if the flow rate is too high, cavitation can occur. To counter that, one can place several rotor in line and split the flow rate. At the very bottom of Figure 4.5 there is the **aspiration tube**, it is a divergent nozzle, since the velocity decreases, the pressure is lower upstream the tube and this sucks water to decrease the distance between shaft and water level which is lost head.

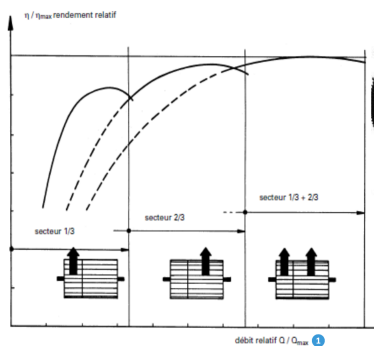


Figure 4.6

Pros and cons:

- + Supports large flow variations.
- + Self-cleaning since everything going in goes out.
- + Easy design, compactness, robustness.
- + Partitioning in sectors to work with high efficiencies over a range of 10%-100% of Q_{max} .
- Rpm is low so must be coupled using gearbox or belt.
- Periodic strike on the blades are source of noise.

4.3 Reaction turbines

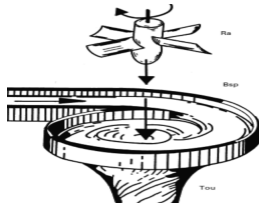


Figure 4.7

A reaction turbine is a closed and immersed device that both uses kinetic energy and pressure difference between the input and output of the rotor. The principle is to create a vortex with the incoming flow and to recover the circular movement of the vortex with the blades, which will deviate the flow so that it becomes parallel to the rotation axis. Be careful with cavitation.

4.3.1 Francis turbines

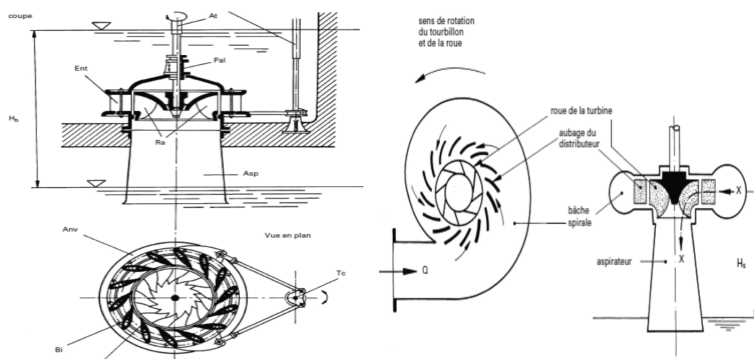


Figure 4.8

The Francis turbine has fixed geometry rotor blades, but movable vanes (changing pitch angle) on the distributor. The flow enters in a spiral casing that will evenly distribute water using the vanes. Again, we have horizontal and vertical configurations. The first is used for low heads and low power while the other for high heads and powers because of high axial thrust and large bearings are required.

It is designed to work on medium heads (3 - 350 m) and medium flows (0.4 to 30 m^3/s) and can develop important power. It has a rpm of 100 to 1000 and can overspeed up to 230%. On the other hand, the design and engineering are very complex requiring the knowledge of group dynamic and ensuring high reliability.

4.3.2 Propeller and Kaplan turbines

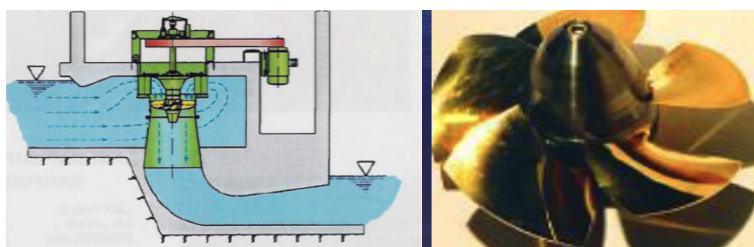


Figure 4.9

These are wheels similar to boat propellers with fixed blades (propeller) or movable (Kaplan). The flow properties (spiral, ...) are similar to the Francis turbine but in Kaplan the flow is purely axial as represented on the figure. The flow is redirected towards the center of the propeller by the fixed or adjustable distributor. When leaving, we have a divergent aspirator to limit turbulences.

These are designed to work on small to medium heads (3-50 m) and high flow rate ($0 - 5 \text{ m}^3/\text{s}$). They are classified according to their provision: bulb turbine, siphon turbine, turbine in S (upstream and downstream), submerged turbine monoblock.

4.3.3 Inverted pumps

These are pumps with inverted flow direction and inverted shaft rotation. Operation similar to the Francis but with lower specific speed and fixed distributor vanes. It is cheap, easy to install and compact. Used for low heads, but has many disadvantages:

- constant flow rate,
- if sudden discharge, high risk of water hammer in the pipe,
- need a flywheel because of fast speed transition,
- additional engineering to make it operational in inverse mode,
- the reversing of the rotation direction takes time,
- lower efficiency than Francis turbine operating in the same conditions.

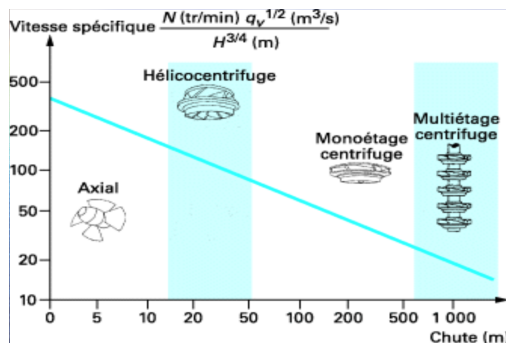


Figure 4.10

4.3.4 Archimedes turbines

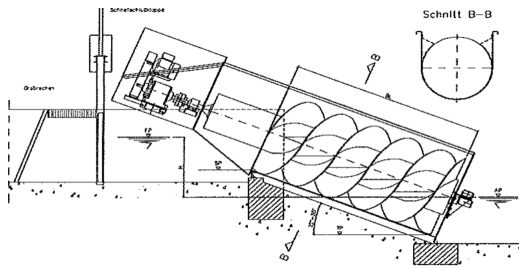
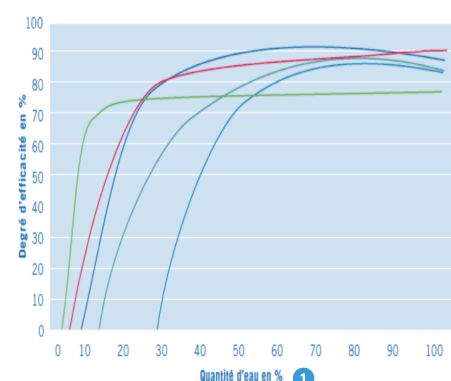


Figure 4.11

Advantages and disadvantages:

- + Compared to other turbines of the same magnitude, the screw has a similar or higher efficiency.
- + Wide range of good efficiency,
- + fish-friendly, no fine grids,
- + robust, simple, not expensive and low maintenance.
- low power, low speed requires multiplier so losses, sealing and lubrication of bottom bearing.

Hydrodynamic screw generates energy by letting the water run into the screw down (it rotates). This is in fact also an inverted pump. It is not submerged and supported by 2 bearings (one of them is thus in the water and is a friction problem). It is used for low head and small or medium flow rates.



42

Figure 4.12

4.4 Performance curves and operating conditions

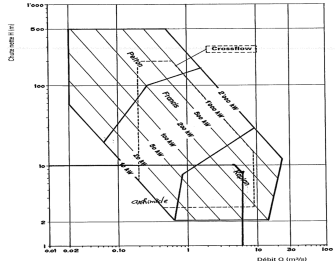


Figure 4.13

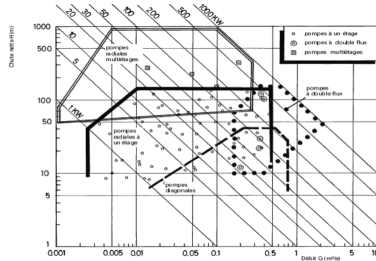


Figure 4.14

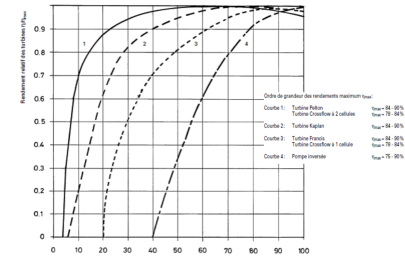


Figure 4.15

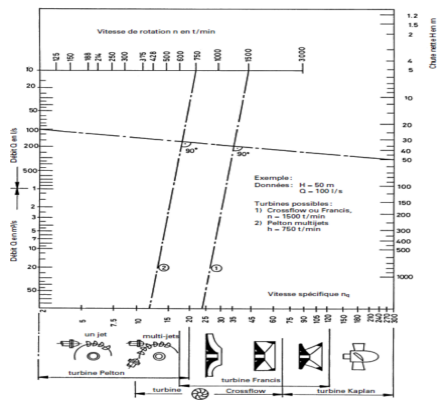


Figure 4.16

The two first figures represent the power curves in function of the head and the flow rate. The third figure shows the efficiency. All what we have discussed previously are summarized here.

The grid has a fixed frequency (50 Hz in Belgium), and thus the maximum rotation speed is limited in function of the number of poles of the generator. It is possible to select the turbine in function of the rotation speed, knowing the flow rate (at left of the graph) and the head (right) as shown on the figure.

4.4.1 Implementation of a hydroturbine

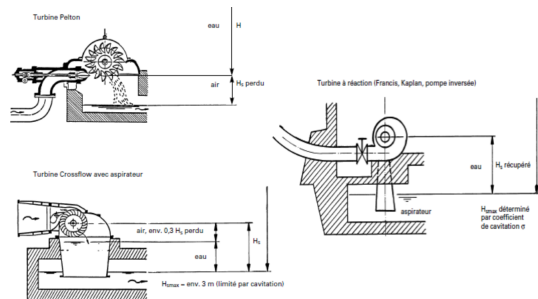


Figure 4.17

This implies that for low head turbines, the location on the circuit may be different from type to type.

We said that the pressure at the entrance of the pump (minimum section) must be higher than the saturation pressure otherwise we have cavitation. We put the pump lower than the upstream water level. Here we introduce the suction head, distance between the central shaft of the turbine and the level of water in the lower reservoir. This suction head is important because it is lost energy in fact. Depending on the type of turbine, the suction head will be different, this is summarized on the figure.

4.4.2 Turbine generator group layout

There are 3 main possibilities: turbine on the shaft of the generator, both with different shafts but directly coupled and the one with the transition of a speed multiplier (belt, gear).

4.5 Summary

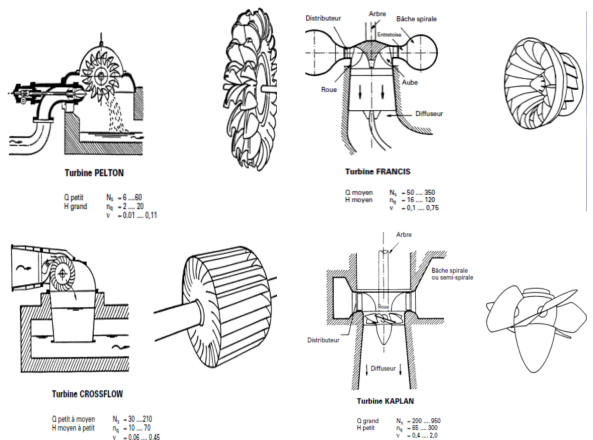


Figure 4.18

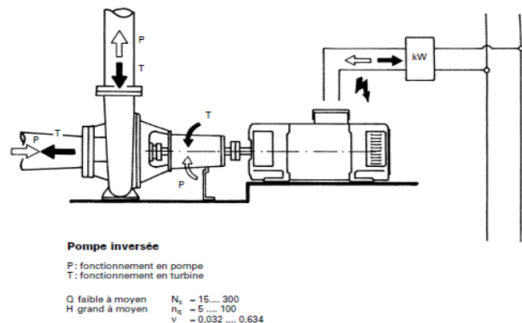


Figure 4.19

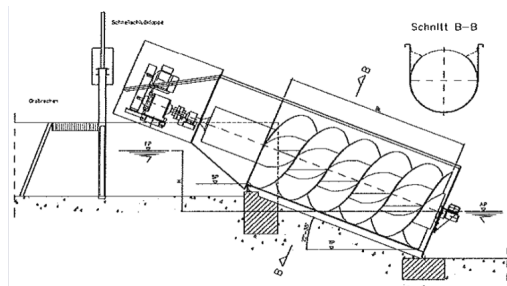


Figure 4.20

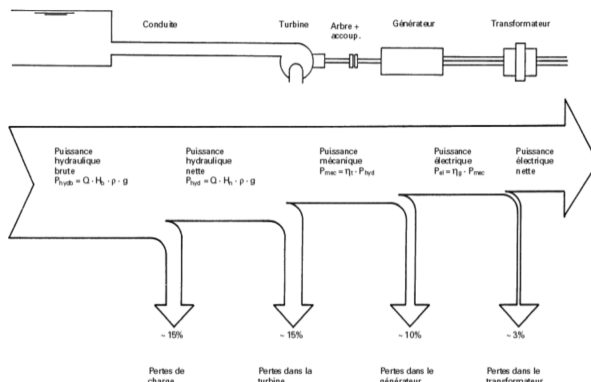


Figure 4.21